

UCLA

UCLA Electronic Theses and Dissertations

Title

Regulation and function of 6-phosphofructo-2-kinase/fructose-2,6-bisphosphatase 3 in innate immune response to viral infection

Permalink

<https://escholarship.org/uc/item/45v4p2fm>

Author

Gold, Sarah

Publication Date

2020

Peer reviewed|Thesis/dissertation

UNIVERSITY OF CALIFORNIA

Los Angeles

Regulation and function of 6-phosphofructo-2-kinase/fructose-2,6-bisphosphatase 3
in innate immune response to viral infection

A dissertation submitted in partial satisfaction
of the requirements for the degree

Doctor of Philosophy in Microbiology, Immunology, and Molecular Genetics

by

Sarah Ruth Gold

2020

© Copyright by
Sarah Ruth Gold
2020

ABSTRACT OF THE DISSERTATION

Regulation and function of 6-phosphofructo-2-kinase/fructose-2,6-bisphosphatase 3
in innate immune response to viral infection

by

Sarah Ruth Gold

Doctor of Philosophy in Microbiology, Immunology, and Molecular Genetics

University of California, Los Angeles, 2020

Professor Genhong Cheng, Chair

In response to viral infection innate immune cells dramatically increase expression of cytokines, interferons, and antiviral genes in a mobilization effort that can include major metabolic reprogramming. How these cells control metabolism and how metabolic pathways themselves serve as generators of immune signals are major questions in immunometabolism. PFKFB3 encodes the metabolic regulatory enzyme phosphofructokinase-2/fructose 2,6-bisphosphatase (PFK-2/FBPase), is induced in response to a variety of stress and inflammatory signals through distinct pathways and has recently been identified as an interferon stimulated gene (ISG). However, the role of interferon in the regulation of PFKFB3 expression has not been clearly established, and PFKFB3's potential functions in antiviral response remain almost entirely unexplored in the literature. We demonstrate here that PFKFB3 is induced in response to either viral infection or viral nucleic acid analogs in a type I interferon-dependent manner. We also found that PFKFB3 induction in response to LPS stimulation similarly requires type I interferon signaling, and that it is potentiated by IL-10 but not Hif1 α in normoxia. PFKFB3 has two major isoforms, A-C-G and A-C-D, the second of which has an alternative C-terminal peptide sequence due to inclusion of a frameshift-generating 23 nt exon D at the 3' end. We designed qPCR primers to quantify induction of PFKFB3's C-D and C-G exon-exon junctions and found that BMDM, MDM and A549 cells all responded to either viral infection or viral nucleic acid analogs by preferentially inducing PFKFB3 A-C-G but not A-C-D or by switching from A-C-D to A-C-G expression. Overexpression of A-C-G

or the truncation mutant A-C, but not A-C-D, inhibited VSV infection in 293T cells; this viral inhibitory effect also depended on PFKFB3 kinase activity and could be conferred via conditioned media but did not depend on an intact nuclear localization signal. Metabolic footprinting by LC/MS indicated increased choline and phosphocholine in the media of 293T cells overexpressing PFKFB3 A-C-G, and addition of choline to cell culture media inhibited VSV infection in a dose-dependent manner. Metabolic profiling by LC/MS of 293T cells overexpressing PFKFB3 isoforms or the A-C truncation mutant demonstrated the expected, increased glycolytic flux phenotype in the A-C-G and A-C but not A-C-D condition, indicating a disabling role for exon D consistent with its lack of viral inhibition. CDP-choline was unexpectedly elevated in tandem with increased glycolysis, and homocysteine levels were increased nearly 100 fold, indicating a severe inhibition or dysfunction of one-carbon metabolism in cells expressing either the fully-active A-C-G isoform or truncation mutant. Finally, we found that PFKFB3 directly binds to and co-precipitates with the outer mitochondrial membrane protein and glycolytic potentiator hexokinase 2 (HK2), in yet another localization for PFKFB3, which is also found in the nucleus and in association with the outer lysosomal membrane.

The dissertation of Sarah Ruth Gold is approved.

Lili Yang

Stephen Smale

Steven J. Bensinger

Genhong Cheng, Committee Chair

University of California, Los Angeles

2020

To a Ms. Sparks, with my apologies

TABLE OF CONTENTS

1 Perspectives on immunometabolism	1
1.1 Introduction	1
1.2 Cell metabolism from a systems perspective	2
1.3 Metabolomics: capabilities and limitations	3
1.4 Multi-level metabolic regulation	4
1.5 Homeostatic adaptation of dynamic systems	5
1.6 PFK-2/FBPase: compact homeostat	6
1.7 PFKFB3 is a glycolytic regulator	7
1.8 Regulation and splicing of PFKFB3	8
1.9 Immunometabolism in innate antiviral response	12
References	14
2 Regulation and function of PFKFB3 in innate immune response to viral infection	20
2.1 Introduction	20
2.2 Results	23
2.2.1 PFKFB3 induction in response to viral infection	23
2.2.2 IFNAR-dependent splicing of PFKFB3 in response to viral infection .	25
2.2.3 Antiviral function of PFKFB3 and its splice isoforms	26
2.2.4 Investigating mechanisms of PFKFB3 antiviral function	27
2.2.5 Effect of PFKFB3 C-terminal peptide sequence on metabolic impact	29
2.2.6 PFKFB3 binds HK2: potential role of PFKFB3 in poly (I:C)-induced hexokinase activity	30

2.3	Discussion	32
2.3.1	Type I interferon signaling mediates preferential induction of the PFKFB3 A-C-G isoform in response to viral infection	32
2.3.2	IL-10 but not Hif1a potentiates IFNAR-dependent induction of PFKFB3 by TLR4	32
2.3.3	Antiviral function of PFKFB3	33
2.3.4	Choline or related metabolites may confer antiviral function in PFKFB3- conditioned media	34
2.3.5	PFKFB3 A-C-G increases intracellular abundance of upper glycolysis reaction products	35
2.3.6	PFKFB3 A-C-G breaks choline and one-carbon metabolism	35
2.3.7	Beyond PFK-2 activity: PFKFB3 binds HK2	37
2.3.8	Conclusions	37
2.4	Methods	39
2.4.1	Cell culture	39
2.4.2	Peripheral Human monocyte-derived macrophages	39
2.4.3	Murine bone marrow-derived macrophages	39
2.4.4	Coimmunoprecipitation	40
2.4.5	Western blot	40
2.4.6	qPCR analysis of gene expression	40
2.4.7	PFKFB3 plasmid constructs	41
2.4.8	Viral infections, flow cytometry and plaque assay	41
2.4.9	Metabolite extraction	41
2.4.10	Ultra-High Performance Liquid Chromatography Mass Spectrometry (UPLC-MS)	42
2.4.11	Choline assay	42

2.5	Figure Legends	44
2.5.1	The type I-specific ISG PFKFB3 is induced in response to viral infection by cytosolic and Toll-like receptors, type I interferon signaling and the cytokine IL-10.	44
2.5.2	Type I interferon-dependent alternative splicing of PFKFB3 in innate antiviral response.	44
2.5.3	PFKFB3 inhibits viral infection dependent on kinase activity and C terminal peptide sequence.	45
2.5.4	PFKFB3-conditioned media confers antiviral effect and PFKFB3 alters metabolic footprint in media.	45
2.5.5	Effects of PFKFB3 C erminal peptide sequence on glycolytic metabolites.	46
2.5.6	Effects of PFKFB3 C-terminal peptide sequence on choline-related metabolites.	46
2.5.7	Co-immunoprecipitation of PFKFB3 isoforms with HK2.	47
	References	55
3	Concluding remarks: implications and future directions	58
3.1	PFKFB3 inhibition: many questions to revisit	58
3.2	PFKFB3, choline and homocysteine converge	59
	References	62

LIST OF FIGURES

1.1	Diagram of PFKFB3 C-terminal exon organization	11
2.1	PFKFB3 is induced in response to viral infection by cytosolic and Toll-like receptors, type I interferon signaling and the cytokine IL-10.	48
2.2	Type I interferon-dependent alternative splicing of PFKFB3 in innate antiviral response.	49
2.3	PFKFB3 inhibits viral infection dependent on kinase activity and C terminal peptide sequence.	50
2.4	PFKFB3-conditioned media confers antiviral effect: possible role for choline.	51
2.5	Effects of PFKFB3 C terminal peptide sequence on glycolytic metabolites.	52
2.6	Effects of PFKFB3 C terminal peptide sequence on choline-related metabolites.	53
2.7	Co-immunoprecipitation of PFKFB3 isoforms with HK2.	54

LIST OF TABLES

1.1	PFKFB3 C-terminal exons	10
2.1	qPCR primer list	43

ACKNOWLEDGMENTS

This work was supported by the T32 Microbial Pathogenesis Training Grant.

I would like to acknowledge the hundreds of mice I have sacrificed, often in vain.

Many thanks to Rosane Teles for human monocytes and to Johanna Scott and the UCLA Metabolomics Center for data acquisition and processing, protocols and support.

More thanks to my research mentor Genhong Cheng for bearing with me, lab members Rogiyh Aliyari, Yao Wang, Kislay Parvatiyar, José Pindado, Natalie Quanquin, Feng Ma, Stephanie Valderramos, and Elisa Deriu for their expertise, to fellow grad students Lotus Loo, Amirali Ghaffari, Shankar Iyer, Anna Reichardt, Gayle Boxx, Maxime Chapon, and Lulan Wang for their camaraderie, to Jingfeng Wang, Shilei Zhang, Bin Hu, and Siwan Wen for being so lovely, to Yucheng Huang for her assistance and to the many lab helpers for keeping everything afloat.

Thank you to Greg Velicer and Kimberly Chen for giving me a shot.

Thank you to my family and especially my husband for abundant patience, and support and love.

VITA

2011 B.S. (Biology) B.A. (Biochemistry, Japanese Language and Culture),
Indiana University

PUBLICATIONS

Zu, S., Deng, Y., Zhou, C. et al. 25-Hydroxycholesterol is a potent SARS-CoV-2 inhibitor. *Cell Res* (2020).

Wu A, Niu P, Wang L, et al. Mutations, Recombination and Insertion in the Evolution of 2019-nCoV. Preprint. *bioRxiv*. (2020)

CHAPTER 1

Perspectives on immunometabolism

1.1 Introduction

A better understanding of cellular metabolism is now increasingly crucial to progress in immunology, from understanding host-pathogen interaction to programming B and T cell biology. The same has been said of cell and molecular biology in general following a resurgence of interest in metabolism after the advent of massively parallel sequencing and genome-wide approaches at the turn of the century (1). Traditional biochemistry triumphed over fifty years ago in the near-complete identification and characterization of the chemical reactions composing cellular metabolism, and for decades after immunology, like cell and molecular biology, dealt with metabolism largely as a black box. Nevertheless, immunologists have found significant crosstalk between immune signaling and metabolic pathways, and within the last decade the field of immunometabolism has formed around a new understanding of metabolic pathways as immune signal generators.

Meanwhile, the field of metabolism has leapt forward from characterizing individual reactions and pathways to understanding, modeling and controlling metabolism as a system. While this approach remains significantly more tractable and profitable in bacteria and yeast (and plants, to some extent), the clear role of metabolic regulation in human cell differentiation and the success of stem cell-enabled cancer immunotherapy in particular highlight the opportunities for network and systems-level understanding of eukaryotic cell metabolism, including metabolic phenotype characterization, metabolic flux analysis and identification of parameters underlying state-switching (2, 3).

The thesis work presented in Chapter 2 is concerned with understanding the regulation

and function of a key metabolic regulatory enzyme, PFKFB3, in the context of innate immune response to viral infection. This work began before the field of immunometabolism had really begun to emerge. It was initially motivated by an interest in understanding metabolism from the host side of host-pathogen interaction, as viruses and other intracellular parasites often reprogram host cell metabolism to support their growth. By this point that interest lies simply in metabolic control, for which the immune response to infection presents a dramatic context: cellular control of metabolism in response to viral infection not only supports antiviral programs, it also maintains stability in the face of often rapid and intense change.

In this introductory chapter I will first describe cell metabolism from a systems perspective, discuss general capabilities and limitations of metabolomics, and introduce biocybernetic adaptive homeostasis concepts to better approach regulation of metabolism in immune response. I will then briefly enumerate the multi-level mechanisms of metabolic regulation before introducing the metabolic regulatory enzyme PFKFB3 and discussing several aspects of its regulation and function. Finally, I will discuss reports of immunometabolic mechanisms relevant to understanding the innate immune response to viral infection.

1.2 Cell metabolism from a systems perspective

Cellular metabolism is the suite of biochemical processes in a cell that either produce energy from the breakdown of molecules or consume energy to do the essential biochemical work of small molecule synthesis, macromolecular polymerization and waste handling. These processes occur via the successive chemical reactions, or metabolic pathways, that together form the cellular metabolic network. A metabolic network is a directed graph in which metabolite nodes are connected by chemical reaction edges. The weights and directions of the edges are determined by the interaction of network dynamics and the underlying Gibbs free energy landscape, so that distinct metastable states, which we refer to as metabolic phenotypes, arise from a single cellular metabolic network via changes in network dynamics (4). A cell may regulate metabolism in such a way as to maintain a metastable state, tightly

controlling dynamics to counter perturbations and maintain homeostasis, or it may actively alter network dynamics to enable switching from one metastable state to another.

Metabolic phenotypes can be characterized via measurements of the metabolome, which is the complete set of small molecule metabolites in a system under a given condition. The term metabolome is meant to imply relation to proteome, transcriptome, and genome, along with many more -omes denoting sets of chemical modifiers, signals, and macromolecules with complex physical arrangement. The components of any or all of these -omes can be thought of as nodes in the connected graph of a system interactome, or set of interactions. The term "fluxome," which refers to the measurement space for metabolic flux analysis, breaks the naming convention because a metabolic flux, or rate of movement through a metabolic pathway, isn't an interactome node. Instead, flux information is useful for understanding and modeling the strength and direction of metabolic network edges.

1.3 Metabolomics: capabilities and limitations

Metabolomics is quantitative metabolic profiling via high resolution mass spectrometry (or NMR spectroscopy, though less commonly used) of intracellular metabolites extracted from cells or tissues. The resulting data illustrates the impact of cell phenotype, manipulation or treatment condition on the relative intracellular pool size of any and all detectable metabolites present in the extract sample. Metabolites extracted from cell media or other milieu can also be measured using the same instrumentation to yield a "footprint" of metabolic activity.

Metabolomic datasets can provide information that complements other -omics data, though integrative data analysis remains challenging. They can also be used to estimate relative metabolic flux through a given pathway, cycle, or portion thereof, and strategic isotopic substrate labeling (ie C13 labelled glucose) in experimental design allows for metabolic flux analysis (MFA), a non-human-intuitive method that relies on computational algorithms to elucidate intracellular flux distribution, or the routing of metabolites and through alternative metabolic pathways (5, 6). Relative changes in metabolite pool sizes and pathway

fluxes are valuable to metabolic pathway modeling and understanding *in vivo*.

Metabolomics capabilities are limited by the sensitivity and resolution of spectrometer instrumentation, the efficiency and usefulness of data analysis algorithms, the need for appropriate chemical standards and for computational time. While these limitations are optimizable, less so are those of due to the diverse nature of metabolites themselves: metabolites vary in their solubility, so that solvent extraction necessarily fails to represent all metabolites in a given sample and some portion of metabolites will be poorly resolved by relatively incompatible chromatography methods. Further, though "real-time" metabolic profiling is possible with direct suspension culture-to-detector instrumentation, in practice sample collection methods are time-consuming and most metabolomic datasets are snapshot measurements of steady state metabolite abundance, possibly at various timepoints (7). This means, however, that we can indulge in metaphor: a metabolic profile can be thought of as akin to a protein crystal structure, so that a metabolic network is like a primary peptide sequence for which the "folding" landscape is enormously complex. Cells have evolved to effectively navigate this landscape, maintaining the ability to switch states— folding and refolding, from the same primary sequence— in response to signaling and changes in the extracellular environment.

1.4 Multi-level metabolic regulation

Cells accomplish stable and efficient responsiveness by regulating metabolism at multiple levels. At the level of physical organization, reactions are localized to cell compartments or condensates, thermodynamic equilibria are altered by active transport of substrates and products across membranes, and pathway intermediates are channeled from one enzyme to the next within metabolons (which may transiently assemble in response to signals or nutrient status, making this regulation physiotemporal.) At the biochemical level metabolic enzyme activity may be positively or negatively regulated by interaction with a substrate, product, or other metabolite, and the enzyme may be post-translationally modified by the covalent addition of a functional group or ubiquitin family protein to affect its activity, conforma-

tion, stability, interaction with other proteins or cellular localization. Finally, cells control metabolism at the level of gene expression: the genes encoding metabolic enzymes are transcriptionally activated and repressed by transcription factors and chromatin modifications, and their transcripts are subject to alternative splicing and RNA interference.

1.5 Homeostatic adaptation of dynamic systems

The phrase "maintain homeostasis" is commonly used in physiology in accordance with the concept of homeostasis as an ideal or stable steady-state around which variance must be controlled. A minimal controls engineering model of a homeostatic regulatory system includes a regulated variable, a variable sensor, an error detector, a controller and an effector. In addition, the model requires a set point value or range of values for the regulated variable. The sensor communicates the value of the regulated variable to the error detector, which compares the sensed value against the variable set point and communicates the error value to the controller. The controller then communicates an output value to the effector that adjusts the variable (8).

The physiologist Walter Cannon coined the term "homeostasis" in 1932 (9). The neurologist Arturo Rosenblueth worked in Cannon's lab but also became involved in the new field of cybernetics, working with mathematician Norbert Wiener and computer engineer Julian Bigelow to understand biological and mechanical self-regulating systems (10). The cyberneticist Ross Ashby, inventor of the Homeostat, further advanced the notion of homeostasis as a dynamic, adaptive process controlling "essential variables" via his theory of ultrastable systems (11). From this perspective, "maintaining homeostasis" more accurately means maintaining the *capability* of a system to self-regulate.

Ashby began as a neuroscientist and psychologist, so his Homeostat looked something like a tiny brain, with four units all connected to one another via electrical inputs and outputs. Each unit housed a current-sensitive, voltage-generating mechanism for which the angle of a pivoting magnet was an essential variable and a 25-position uniselector switch to convert any unit-generated voltage into one of 25 possible randomly-selected current feedback outputs.

Perturbation of the magnet angle on any unit perturbed the system's dynamic equilibrium, inducing new currents that changed magnet angles and initiated uniselector state-search in all . The system was designed to be an exemplar of Ashby's ultrastability concept and as such was given more than adequate requisite variety: with eight current input parameters (resistance and capacitance) and 25 uniselector settings for each of the four units, the number of possible controller states (25^4) far exceeded the number of system states (32) (12).

The Homeostat was both small and physically unwieldy, and attempts to scale into larger analog computers failed. However, its fully-connected network topology made it a complex dynamic, resonant system with emergent sensor, error detector and effector functions, and much more relevant to understanding homeostasis via intracellular interaction networks than individual engineering control circuits.

1.6 PFK-2/FBPase: compact homeostat

PFKFB1-4 all encode isozymes of 6-phosphofructo-2-kinase/fructose 2,6-bisphosphatase (PFK-2/FBPase), a bifunctional enzyme that interconverts fructose 6-phosphate and fructose 2,6-bisphosphate via the enzymatic activity of N-terminal kinase and C-terminal bisphosphatase domains. These isozymes differ in their regulation, tissue expression, and enzyme kinetics, but they all control the same two metabolite pools: fructose 6-phosphate, for use in glycolysis or the pentose phosphate pathway, and fructose 2,6-bisphosphate, an allosteric activator of phosphofructokinase (PFK-1), which converts fructose 6-phosphate to fructose 1,6-bisphosphate in the committed step of glycolysis.

From a homeostatic point of view, PFK-2/FBPases control the fructose 6-phosphate pool they share with PFK-1 like compact homeostats. They simultaneously "sense" and "compare" fructose 6-phosphate and fructose 2,6-bisphosphate pool sizes and "effect" adjustment via dual activities, with kinase to phosphatase activity ratios governing the range outside of which an energetic "error" is detected in the relative size of the fructose 6-phosphate pool. A low kinase to phosphatase ratio allows for a large pool of fructose 6-phosphate to accumulate. At a 1:1 ratio, the size of either pool is limited by whatever concentration of fructose

2,6-bisphosphate is necessary to allosterically activate PFK-1. (That concentration could be exceedingly low vs total cell volume if substrate channeling were facilitated in a metabolon.) A high kinase to phosphatase ratio would allow for a large pool of fructose 2,6-bisphosphate to accumulate even as the fructose 6-phosphate pool remained small.

Kinase to phosphatase activity ratios can be dynamically regulated by differential isozyme expression: the AMPK-activated *in vitro* activity ratio of the PFKFB3 isozyme is so high (700:1) that in comparison to other PFK-2/FBPase-2 isozymes (0.1:1-10:1), PFKFB3 may be thought to essentially function as a kinase (13). On the other hand, TIGAR (Tp53-induced Glycolysis and Apoptosis Regulator) encodes only a fructose 2,6-bisphosphatase, with protein sequence similarity to the FBPase-2 domains of PFKFB1-4. While the (mostly) kinase and a bisphosphatase might appear to be at odds, experimental evidence strongly suggests that they play a more complementary role: knockdown of PFKFB3 induced TIGAR expression in HeLa cells while knockdown of TIGAR induced PFKFB3 expression in primary human leukemia cells (14, 15). Interestingly, Cheung et al reported that TIGAR localizes to the mitochondria and stimulates the mitochondrial hexokinase HK2 under hypoxic conditions, independent of bisphosphatase activity (16).

1.7 PFKFB3 is a glycolytic regulator

Glycolytic enzymes and related regulatory enzymes present attractive cancer drug targets because many cancer cells exhibit a pattern of metabolism often called the Warburg effect, or increased glucose flux through glycolysis and limited oxidative phosphorylation even in the presence of sufficient oxygen. PFKFB3 is expressed in many tumor types and is regarded as an "on switch" for Warburg metabolism, generating the allosteric activator fructose 2,6-bisphosphate to increase PFK-1 activity and glycolytic flux (although increased glycolytic flux may largely be due to an increased glucose uptake controlled by hexokinase and glucose transporters) (17, 18). Activated M1 macrophages and other myeloid cells share metabolic similarity to cancer cells, exhibiting a preference for glycolysis even in the presence of adequate oxygen. Accordingly, LPS-activated macrophages upregulate PFKFB3 (19).

1.8 Regulation and splicing of PFKFB3

PFKFB3 is confined to the cytosol by acetylation at lysine 472 that interferes with its nuclear localization signal (20). Methylation at arginines 131 and 134 protects PFKFB3 from proteasomal degradation subsequent to ubiquitination by the E3 ubiquitin ligase APC/C-Cdh1, which also targets cell cycle proteins (21–23).

PFKFB3 kinase is activated by AMP-activated protein kinase (AMPK) phosphorylation at S461 and inhibited by the glycolytic intermediate phosphoenolpyruvate (PEP), the substrate of pyruvate kinase (24, 25). Interestingly, it is also inhibited by a product of pyruvate kinase, L-2-phospholactate (2P-lactate), which is formed by pyruvate kinase acting on L-lactate in an "erroneous" but thermodynamically favorable side reaction. The metabolite repair enzyme phosphoglycolate phosphatase (PGP) can dephosphorylate 2P-lactate to relieve this inhibition (26).

PFKFB3 expression is induced in response to diverse stimuli via distinct signaling pathways and transcription factors. PFKFB3 expression could be directly induced by the peptide hormone PACAP in a PKC-dependent manner in the AR4-2J rat pancreatic carcinoma cell line and by progestin stimulation in the T-47D, MCF-7 and MDA-MB-231 human breast cancer cell lines (27, 28). It can be induced in hypoxic conditions via the oxygen-inhibited transcription factor Hif1a (24) and by osmotic or oxidative stress or DNA damage via p38/MAPK (29). It is induced (along with hexokinase 2) in response to IL-6 both in MEFS and in early stage colorectal cancer (30, 31) PFKFB3 was found to be induced in a diabetic mouse liver model via PI3K-Akt-mTOR proliferative signaling (32) and was recently found to be induced in response to misfolded protein stress caused by islet amyloid polypeptide plaques of β -cells in type II diabetes (33). It is induced by mTOR in acute myeloid leukemia (34). It is induced by overexpression of the transcription factor E2F1 (35) and repressed by the tumor suppressor p53 (36).

Like many genes, PFKFB3 mRNA is alternatively spliced to produce multiple isoforms (Figure 1.1) The 3' ends of PFKFB3 mRNA are spliced in a tissue-specific manner and in response to a variety of stimuli. The two major splice isoforms of PFKFB3 are often termed

the "ubiquitous" uPFK-2, and the "inducible" iPFK-2, because splicing-agnostic PFKFB3 had been previously termed iPFK-2 (37–40). The 3' exons are also referred to as exons A through G to make comparison of mouse, human and rat isoforms easier (see Table 1.1) Exon A is 65 nt and constitutively expressed. Exon B is 87 nt and is expressed in rodents but leads to nonsense-mediated decay in humans. Exon C is 174 nt and contains a nuclear localization signal (41, 42). Exon D is only 23 nt and causes a frameshift leading to a different C terminal protein sequence (Figure 1.1) Exons E (53 nt) and F (43 nt) seem to be specific to brain. Exon G is 3114 nt, contains both coding sequence and the 3' UTR, and is constitutively expressed but translated differently if Exon D is present. Using the lettering convention above, uPFK-2 is PFKFB3-A-C-G, while iPFK-2 is PFKFB3-A-C-D-G, or A-C-D to emphasize the effect on the protein product. In human brain tissues these isoforms have been referred to as UBI2K5 and UBI2K4, respectively (43).

Alternative splicing of PFKFB3 and the effects of its splice isoforms have been explored to limited extent in cancer and other disease states (18). Zscharnack et al. investigated alternative splicing in astrocytomas, finding that diversity of splice isoforms diminished as a function of clinical severity, with high grade astrocytomas differing from low grade in that the percentage of high grade astrocytomas expressing only the UBI2K5 and UBI2K6 (A-G and A-C-G) isoforms was nearly double that of low grade astrocytomas (only 10% of control tissue samples lacked isoforms with exon D) (44). They observed increased cellular fructose 2,6-bisphosphate levels after overexpressing each of the PFKFB3 isoforms in the U87 glioma cell line but found that the A-G and A-C-G, but not A-C-D, isoforms increased lactate significantly. Instead, they found that the overexpressed A-C-D form decreased total cell number and cell viability, and that UBI2K4 (A-C-D) expression levels positively correlated with doubling time in a panel of human cancer cell lines. However, PFKFB3 splice isoforms have not been characterized in antiviral immune response.

Exon name	Length (nt)	Expression and features
A	65	Constitutively expressed
B	87	Inclusion causes nonsense-mediated decay in human (expressed in mouse)
C	174	Frequently expressed. Contains nuclear localization signal
D	23	Inclusion causes frameshift and alternate C-terminal protein sequence
E	53	Specific to brain. Co-occurs with Exon D.
F	43	Specific to brain. Co-occurs with Exon D.
G	3114	Constitutively expressed. Contains coding sequence (translation determined by upstream exon inclusion) and 3' UTR

Table 1.1: PFKFB3 C-terminal exons

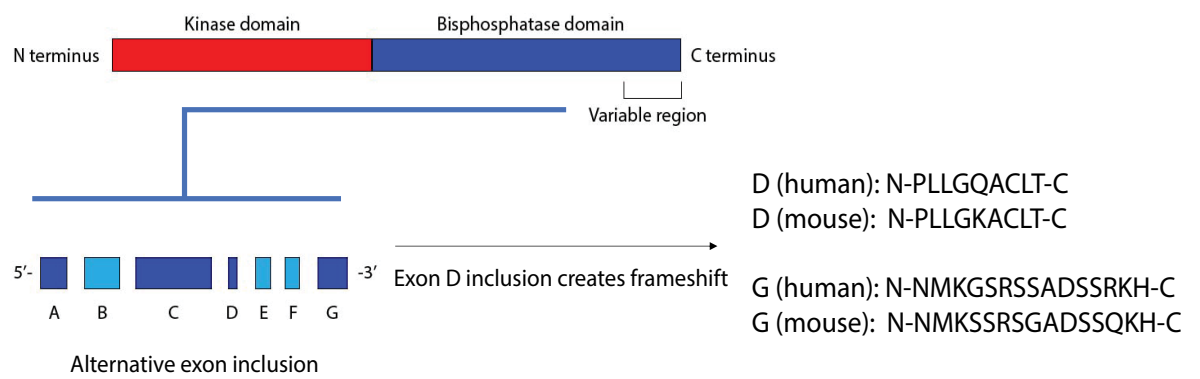


Figure 1.1: Diagram of PFKFB3 C-terminal exon organization

1.9 Immunometabolism in innate antiviral response

Reports of innate immunometabolism are increasingly numerous but have largely been concerned with metabolic reprogramming in the proinflammatory or alternative activation of dendritic cells and macrophages (45). There are, however, some key results to highlight regarding innate antiviral immunometabolism. From two perspectives on cholesterol synthesis in antiviral response, Liu et al found that cholesterol-25 hydroxylase is an ISG that can broadly inhibit viral infection via its product 25HC (46), while York et al found that, in a true immunometabolic homeostasis control circuit, type I interferon signaling both limits cholesterol synthesis via effects on genes in the mevalonate pathway and is induced in response to decrease in the ER cholesterol pool that influences STING/TBK1 to effect subsequent phosphorylation of the interferon response factor IRF3 (47).

STING also comes into play in a potential feedback loop between type I interferon and itaconate, the "poster child of metabolic reprogramming" (48). Interferon response gene I (IRG1), the gene most strongly induced by LPS stimulation in macrophages, has been renamed ACOD1 to reflect its recently-discovered identity as aconitate decarboxylase, an enzyme that converts the TCA cycle intermediate aconitate into the antimicrobial and immunoregulatory metabolite itaconate. Type I interferon signaling induces ACOD1 expression and itaconate production, which in turn activates the anti-inflammatory activity of NRF2 (49), and cell-permeable itaconate derivatives have been shown to repress STING and type I interferon signaling in response to viral infection in an NRF2-dependent manner (50).

Finally, systems approaches are a promising route for further discovery of innate immunometabolism relevant to viral infection. Passalacqua et al recently performed metabolomic and energetic profiling of norovirus-infected RAW 264.7 cells, finding elevated glycolysis mediated by Akt but not type I interferon that potentiated norovirus infection (51). Zhang et al performed metabolomic profiling over a timecourse of RIG-1/MAVS activation by poly (I:C) in HEK293 cells and found early, transient reduction in glycolysis. They showed that increased media glucose was negatively correlated with IFN β production and resistance to VSV infection, indicating that a transient reduction in glycolysis removed a barrier to type I

interferon response downstream of MAVS. They then demonstrated that the RIG-1 adaptor MAVS interacts with the mitochondrial hexokinase HK2, a major regulator of glycolysis, until RIG-I becomes engaged by poly (I:C) and provided evidence that the glycolysis product lactate might directly bind MAVS to prevent basal MAVS/RIG-I interaction (52). Localization, protein-protein interactions and metabolite-protein interactions are exciting areas for further exploration of immunometabolic crossregulation and control.

REFERENCES

1. McKnight, S. L. On Getting There from Here. *Science* **330**, 1338–1339. ISSN: 0036-8075 (2010).
2. Kawalekar, O. U. *et al.* Distinct Signaling of Coreceptors Regulates Specific Metabolism Pathways and Impacts Memory Development in CAR T Cells. *Immunity* **44**, 380–390. ISSN: 1074-7613 (2016).
3. Xu, X., Gnanaprakasam, J. N. R., Sherman, J. & Wang, R. A Metabolism Toolbox for CAR T Therapy. *Frontiers in Oncology* **9**, 322. ISSN: 2234-943X (2019).
4. Martino, D. D., Figliuzzi, M., Martino, A. D. & Marinari, E. A Scalable Algorithm to Explore the Gibbs Energy Landscape of Genome-Scale Metabolic Networks. *PLoS Computational Biology* **8**, e1002562. ISSN: 1553-734X. eprint: 1206.5092 (2012).
5. Sims, J. K., Manteiga, S. & Lee, K. Towards high resolution analysis of metabolic flux in cells and tissues. *Current Opinion in Biotechnology* **24**, 933–939. ISSN: 0958-1669 (2013).
6. Zamboni, N., Saghatelian, A. & Patti, G. J. Defining the Metabolome: Size, Flux, and Regulation. *Molecular Cell* **58**, 699–706. ISSN: 1097-2765 (2015).
7. Link, H., Fuhrer, T., Gerosa, L., Zamboni, N. & Sauer, U. Real-time metabolome profiling of the metabolic switch between starvation and growth. *Nature Methods* **12**, 1091–1097. ISSN: 1548-7091 (2015).
8. Modell, H. *et al.* A physiologist’s view of homeostasis. *Advances in Physiology Education* **39**, 259–266. ISSN: 1043-4046 (2015).
9. Cannon, W. *The wisdom of the body.* (W W Norton & Co, 1932).
10. Goldstein, D. S. & Kopin, I. J. Homeostatic systems, biocybernetics, and autonomic neuroscience. *Autonomic Neuroscience* **208**, 15–28. ISSN: 1566-0702 (2017).
11. Williams, H. *Homeostatic Adaptive Networks* PhD thesis (2006).

12. Cariani, P. A. The homeostat as embodiment of adaptive control. *International Journal of General Systems* **38**, 139–154. ISSN: 0308-1079 (2009).
13. Clark, J. Enzyme kinetics : 6-phosphofructo-2-kinase/2,6-bisphosphatase. (2014).
14. Qian, S. *et al.* TIGAR cooperated with glycolysis to inhibit the apoptosis of leukemia cells and associated with poor prognosis in patients with cytogenetically normal acute myeloid leukemia. *Journal of Hematology & Oncology* **9**, 128 (2016).
15. Simon-Molas, H. *et al.* Akt mediates TIGAR induction in HeLa cells following PFKFB3 inhibition. *FEBS Letters* **590**, 2915–2926. ISSN: 1873-3468 (2016).
16. Cheung, E. C., Ludwig, R. L. & Vousden, K. H. Mitochondrial localization of TIGAR under hypoxia stimulates HK2 and lowers ROS and cell death. *Proceedings of the National Academy of Sciences* **109**, 20491–20496. ISSN: 0027-8424 (2012).
17. Shi, L., Pan, H., Liu, Z., Xie, J. & Han, W. Roles of PFKFB3 in cancer. *Signal Transduction and Targeted Therapy* **2**, 17044. ISSN: 2095-9907 (2017).
18. Bartrons, R. *et al.* Fructose 2,6-Bisphosphate in Cancer Cell Metabolism. *Frontiers in Oncology* **8**, 331. ISSN: 2234-943X (2018).
19. Ruiz-Garcia, A. *et al.* Cooperation of Adenosine with Macrophage Toll-4 Receptor Agonists Leads to Increased Glycolytic Flux through the Enhanced Expression of PFKFB3 Gene. English. *The Journal of biological chemistry* **286**, 19247–19258 (2011).
20. Li, F.-L. *et al.* Acetylation accumulates PFKFB3 in cytoplasm to promote glycolysis and protects cells from cisplatin-induced apoptosis. *Nature Communications* **9**, 508 (2018).
21. Yamamoto, T. *et al.* Reduced methylation of PFKFB3 in cancer cells shunts glucose towards the pentose phosphate pathway. English. *Nature communications* **5** (2014).
22. Almeida, A., Bolaños, J. P. & Moncada, S. E3 ubiquitin ligase APC/C-Cdh1 accounts for the Warburg effect by linking glycolysis to cell proliferation. *Proceedings of the National Academy of Sciences* **107**, 738–741. ISSN: 0027-8424 (2010).

23. Riera, L. *et al.* Regulation of ubiquitous 6-phosphofructo-2-kinase by the ubiquitin-proteasome proteolytic pathway during myogenic C2C12 cell differentiation. *FEBS Letters* **550**, 23–29. ISSN: 0014-5793 (2003).
24. Marsin, A.-S., Bouzin, C., Bertrand, L. & Hue, L. The Stimulation of Glycolysis by Hypoxia in Activated Monocytes Is Mediated by AMP-activated Protein Kinase and Inducible 6-Phosphofructo-2-kinase. *Journal of Biological Chemistry* **277**, 30778–30783. ISSN: 0021-9258 (2002).
25. Almeida, A., Moncada, S. & Bolaños, J. P. Nitric oxide switches on glycolysis through the AMP protein kinase and 6-phosphofructo-2-kinase pathway. *Nature Cell Biology* **6**, 45–51. ISSN: 1465-7392 (2004).
26. Collard, F. *et al.* A conserved phosphatase destroys toxic glycolytic side products in mammals and yeast. *Nature Chemical Biology* **12**, 601–607. ISSN: 1552-4450 (2016).
27. Schäfer, H., Trauzold, A., Siegel, E. G., Fölsch, U. R. & Schmidt, W. E. PRG1: a novel early-response gene transcriptionally induced by pituitary adenylate cyclase activating polypeptide in a pancreatic carcinoma cell line. *Cancer research* **56**, 2641–8. ISSN: 0008-5472 (1996).
28. Hamilton, J. A., Callaghan, M. J., Sutherland, R. L. & Watts, C. K. W. Identification of PRG1, A Novel Progestin-Responsive Gene with Sequence Homology to 6-Phosphofructo-2-Kinase/Fructose- 2,6-Bisphosphatase. *Molecular Endocrinology* **11**, 490–502. ISSN: 0888-8809 (1997).
29. Novellademunt, L. *et al.* PFKFB3 activation in cancer cells by the p38/MK2 pathway in response to stress stimuli. English. *The Biochemical journal* **452**, 531–543 (2013).
30. Ando, M. *et al.* Interleukin 6 Enhances Glycolysis through Expression of the Glycolytic Enzymes Hexokinase 2 and 6-Phosphofructo-2-kinase/Fructose-2,6-bisphosphatase-3. *Journal of Nippon Medical School* **77**, 97–105. ISSN: 1345-4676 (2010).
31. HAN, J. *et al.* Interleukin-6 stimulates aerobic glycolysis by regulating PFKFB3 at early stage of colorectal cancer. *International Journal of Oncology* **48**, 215–224. ISSN: 1019-6439 (2015).

32. Duran, J. *et al.* Pfkfb3 is transcriptionally upregulated in diabetic mouse liver through proliferative signals. *FEBS Journal* **276**, 4555–4568. ISSN: 1742-4658 (2009).
33. Montemurro, C. *et al.* IAPP toxicity activates HIF1 α /PFKFB3 signaling delaying β -cell loss at the expense of β -cell function. *Nature Communications* **10**, 2679 (2019).
34. Feng, Y. & Wu, L. mTOR up-regulation of PFKFB3 is essential for acute myeloid leukemia cell survival. *Biochemical and Biophysical Research Communications* **483**, 897–903. ISSN: 0006-291X (2017).
35. Almacellas, E. *et al.* PHOSPHOFRUCTOKINASES AXIS CONTROLS GLUCOSE-DEPENDENT mTORC1 ACTIVATION DRIVEN BY E2F1. *iScience* **20**, 434–448. ISSN: 2589-0042 (2019).
36. Franklin, D. A. *et al.* p53 coordinates DNA repair with nucleotide synthesis by suppressing PFKFB3 expression and promoting the pentose phosphate pathway. *Scientific Reports* **6**, 38067 (2016).
37. Chesney, J. *et al.* An inducible gene product for 6-phosphofructo-2-kinase with an AU-rich instability element: role in tumor cell glycolysis and the Warburg effect. English. *Proceedings of the National Academy of Sciences of the United States of America* **96**, 3047–3052 (1999).
38. Navarro-Sabaté, À. *et al.* The human ubiquitous 6-phosphofructo-2-kinase/fructose-2,6-bisphosphatase gene (PFKFB3): promoter characterization and genomic structure. English. *Gene* **264**, 131–138 (2001).
39. Mahlknecht, U., Chesney, J., Hoelzer, D. & Bucala, R. Cloning and chromosomal characterization of the 6-phosphofructo-2-kinase/fructose-2,6-bisphosphatase-3 gene (PFKFB3, iPFK2). *International Journal of Oncology* **23**, 883–891 (2003).
40. Duran, J. *et al.* Overexpression of ubiquitous 6-phosphofructo-2-kinase in the liver of transgenic mice results in weight gain. *Biochemical and Biophysical Research Communications* **365**, 291–297. ISSN: 0006-291X (2008).

41. Yalcin, A. *et al.* Nuclear targeting of 6-phosphofructo-2-kinase (PFKFB3) increases proliferation via cyclin-dependent kinases. English. *The Journal of biological chemistry* **284**, 24223–24232 (2009).
42. Yalcin, A. *et al.* 6-Phosphofructo-2-kinase (PFKFB3) promotes cell cycle progression and suppresses apoptosis via Cdk1-mediated phosphorylation of p27. English. *Cell Death & Disease* **5**, e1337 (2014).
43. Kessler, R. & Eschrich, K. Splice isoforms of ubiquitous 6-phosphofructo-2-kinase/fructose-2,6-bisphosphatase in human brain. English. *Molecular Brain Research* **87**, 190–195 (2001).
44. Zscharnack, K., Kessler, R., Bleichert, F., Warnke, J. P. & Eschrich, K. The PFKFB3 splice variant UBI2K4 is downregulated in high-grade astrocytomas and impedes the growth of U87 glioblastoma cells. English. *Neuropathology and Applied Neurobiology* **35**, 566–578 (2009).
45. Bossche, J. V. d., O’Neill, L. A. & Menon, D. Macrophage Immunometabolism: Where Are We (Going)? *Trends in Immunology* **38**, 395–406 (2017).
46. Liu, S.-Y. *et al.* Interferon-Inducible Cholesterol-25-Hydroxylase Broadly Inhibits Viral Entry by Production of 25-Hydroxycholesterol. English. *Immunity* **38**, 92–105 (2013).
47. York, A. G. *et al.* Limiting Cholesterol Biosynthetic Flux Spontaneously Engages Type I IFN Signaling. English. *Cell* **163**, 1716–1729 (2015).
48. O’Neill, L. A. J. & Artyomov, M. N. Itaconate: the poster child of metabolic reprogramming in macrophage function. *Nature Reviews Immunology* **19**, 273–281. ISSN: 1474-1733 (2019).
49. Mills, E. L. *et al.* Itaconate is an anti-inflammatory metabolite that activates Nrf2 via alkylation of KEAP1. *Nature* **556**, 113–117. ISSN: 0028-0836 (2018).
50. Olganier, D. *et al.* Nrf2 negatively regulates STING indicating a link between antiviral sensing and metabolic reprogramming. *Nature Communications* **9**, 3506 (2018).

51. Passalacqua, K. D. *et al.* Glycolysis Is an Intrinsic Factor for Optimal Replication of a Norovirus. *mBio* **10**, e02175–18 (2019).
52. Zhang, W. *et al.* Lactate Is a Natural Suppressor of RLR Signaling by Targeting MAVS. *Cell* **178**, 176–189.e15. ISSN: 0092-8674 (2019).

CHAPTER 2

Regulation and function of PFKFB3 in innate immune response to viral infection

2.1 Introduction

PFKFB3 encodes an isozyme of the metabolic regulator phosphofructokinase-2/fructose 2,6-bisphosphatase (PFK-2/FBPase) that increases the cellular pool of fructose 2,6-bisphosphate, an allosteric regulator of the glycolytic enzyme fructokinase (PFK-1). Despite being a dual-functioning enzyme, a high relative kinase to phosphatase activity ratio (700:1) makes PFKFB3 function essentially as a kinase, so that PFKFB3 has been viewed as a switch to turn on glycolysis (1). PFKFB3 is also expressed in many cancer cell types, and so has been an attractive target for controlling the classic Warburg aerobic glycolysis phenotype. However, PFKFB3 may have a broader range of functions than control of glycolysis, as it has recently been found to activate nuclear cyclin-dependent kinases (2) and to interact with PFK-1 and Ragulator proteins at the lysosome (3). Indeed, PFKFB3 expression is induced by a variety of proinflammatory stimuli via distinct signaling pathways, suggesting potentially variable or signal-specific functions that may be mediated by expression of alternatively spliced isoforms.(4).

PFKFB3 is also known to be an interferon-stimulated gene (ISG). However, the role of interferons in the regulation of PFKFB3 has not been clearly established, and PFKFB3's potential functions in antiviral response remain almost entirely unexplored in the literature. Recently, Jiang et al showed that that VSV infection increased glycolysis in an interferon-dependent manner in macrophages (but not MEFs) and that glycolysis supported the capacity of macrophages to phagocytose virus-infected cells (5). They further showed that

interferon treatment could increase PFKFB3 expression, that increased PFKFB3 expression increased glycolysis as expected, and that RSV-A2 infection was moderately amplified in heterozygous KO PFKFB3^{+/-} mice (homozygous PFKFB3 KO mice have an embryonic lethal phenotype) (6).

Liu et al first identified PFKFB3 as a potential type I interferon-induced, antiviral factor using a FACS-based antiviral screen of genes induced by interferon stimulation in bone marrow derived macrophages (BMDM) (7). PFKFB3 was specifically induced by type I but not type II interferon in the initial whole-genome microarray experiment. The signal intensity of fluorescent oligonucleotide probes targeting PFKFB3 was increased in samples from BMDMs treated with a representative type I interferon (recombinant murine IFN α -4), but not the type II interferon gamma (IFN γ , Figure 2.1 A). Moreover, neither type I nor type II interferon treatment increased signal intensity from probes targeting the PFK-2/FBPase isozymes PFKFB1, PFKFB2, or PFKFB4. Immune responses in mice or mouse cells can differ significantly from the human immune responses they are meant to model, but the same specificity of response to type I but not type II interferon can be seen in publicly available RNA-seq data for human monocyte-derived macrophages (MDMs) treated with IFN β or IFN γ (Figure 2.1 B, data accessible at NCBI GEO database, accessions GSE82227 and GSE125352) (8, 9).

Here we further investigate the regulation and function of PFKFB3 in innate immune response to viral infection, making use of gene expression studies, viral infection assays, metabolomics and in vitro assays to establish a role for both PFKFB3 kinase activity and C-terminal peptide sequence, determined by preferential isoform induction, in the antiviral and metabolic impacts of PFKFB3. Making use of gene knockout BMDM, we first establish type I interferon signaling upstream of PFKFB3 induction in response to viral infection or viral nucleic acid analogs, establish a role for IL-10 in PFKFB3 induction, and discover the preferential induction of PFKFB3's A-C-G splice isoform in response to these signals via qPCR amplification of exon-exon junctions. Making use of PFKFB3 isoform and mutant plasmid constructs, we demonstrate the requirement for kinase activity in PFKFB3 antiviral function and the null function of the A-C-D isoform. We investigate the mecha-

nism of PFKFB3 antiviral function further, finding a possible role for choline as an antiviral metabolite supplement. Using LC/MS-based metabolomics, we find that the A-C-D isoform is again null for the glycolytic phenotype induced by PFKFB3 A-C-G, and also find that PFKFB3-induced glycolysis is accompanied by dramatic increases in CDP-choline and homocysteine, indicating inhibition of one-carbon metabolism. We further show that PFKFB3 binds the mitochondrial hexokinase 2 (HK2), suggesting further routes of investigation in understanding this important metabolic regulator.

2.2 Results

2.2.1 PFKFB3 induction in response to viral infection

Importantly, no direct link has yet been shown between IFNAR, PFKFB3 and viral infection. We therefore began by infecting WT and IFNAR1 KO BMDM with VSV-GFP at an MOI of 5.0. We analyzed relative PFKFB3 induction by qPCR 6 hours after infection using primers that amplify constitutively expressed exons and found that BMDM upregulate expression of PFKFB3 in response to VSV infection only if the type I interferon receptor is intact (Figure 2.1 C), indicating that PFKFB3 not just a nominal ISG but is in fact induced in the interferon-driven response to actual viral infection.

Type I interferon genes are induced in response to the molecular signals of infection often referred to as pathogen-associated molecular patterns (or PAMPs.) Cells can induce type I interferon in response to both RNA and DNA viruses via phosphorylation and nuclear translocation of the interferon response factor IRF3 by the downstream effector TBK1, but they are sensed by different cytosolic receptors. Cytosolic RNA and DNA, which can be mimicked by transfection of the viral RNA analog poly (I:C) and the viral DNA analog poly (dA:dT), are detected by the dsRNA helicases RIG-1 and MDA5 (with the help of adaptor MAVS) and the enzyme cGAS (with its adaptor STING), respectively. We transfected the human A549 cell line with poly (I:C) and poly (dA:dT) for 24 hours and saw increased PFKFB3 protein expression in response to both viral nucleic acid analogs (Figure 2.1 D).

Viral RNA and DNA or their analogs can also be sensed by Toll-like receptors at the cell surface or in endosomes. Without the help of a transfection reagent, internalized poly (I:C) cannot escape the endosomal compartment and is primarily sensed by the Toll-like receptor TLR3, which uses the adaptor TRIF to effect downstream signaling leading to interferon induction. TLR4, which primarily detects lipopolysaccharide (LPS) in the membranes of gram-negative bacteria, uses both TRIF and MyD88 as adaptors, while TLR2 (in complex with either TLR1 or TLR6) uses MyD88 but not TRIF. To investigate the regulation of PFKFB3 downstream of Toll-like receptors, we stimulated WT and TRIF KO BMDMs for 16 hours with the purified bacterial lipopolysaccharide component Lipid A, Poly (I:C), or

the TLR1/2 agonist Pam3CSK4 and extracted whole cell lysates. Western blot for PFKFB3 indicated increased PFKFB3 expression at the protein level in response to Lipid A and Poly (I:C) but not Pam3CSK4 that was lost in the absence of TRIF (Figure 2.1 E.) We also stimulated these cells with the pseudo-hypoxic Hif1 α stabilizer DMOG as a control, finding that in BMDM, while Lipid A stimulation increased expression of both Hif1 α and PFKFB3, DMOG induced Hif1 α accumulation independently of TRIF, and Hif1 α did not accumulate in response to poly(I:C) stimulation.

Cells release interferons into the extracellular environment, where interferon receptors on the extracellular surface sense the autocrine or paracrine signal to effect a JAK/STAT phosphorylation cascade leading to nuclear translocation of STAT and induction of target genes. Type I interferons cause major shifts in gene expression, with rapid and sustained induction of antimicrobial and inflammatory response that nevertheless must eventually be resolved. The cytokine IL-10 is induced by type I interferon and plays a key role in resolution of inflammation (10). Because PFKFB3 expression peaks later after stimulation than typical ISGs, we wondered if IL-10 might play a role in regulating PFKFB3 expression.

We stimulated WT, IFNAR1 KO and IL-10 KO BMDM with 100 ng/mL Lipid A for 6 hours and quantified relative PFKFB3 induction by qPCR, finding that BMDMs no longer upregulate expression of PFKFB3 in response to Lipid A if IL-10 is lost (Figure 2.1 F). It was unclear why IL-10 would be required for PFKFB3 induction, so we asked if related metabolic genes might also be affected. The STRING gene interaction network for PFKFB3 is largely defined by the substrate fructose 6-phosphate (shared by PFKL, PFKM, PFKP, PFKFB1, PFKFB2, PFKFB4, and MPI) and the substrate fructose 2,6-bisphosphate (shared by PFKFB1-4 and TIGAR.) Interestingly, the hexokinase genes HK1, HK2 and HK3 are also in this network. We accessed publicly available whole-genome microarray data for human PBMCs stimulated with IL-10 and analyzed the effect of IL-10 on the expression of genes within the interaction network (Figure 2.1 G, data accessible at NCBI GEO database, accession GSE43700) (9, 11). In response to IL-10 stimulation, PBMCs significantly upregulated PFKFB3, TIGAR and HK3, while downregulating HK2.

Taken together these data indicate that the type I interferon-specific ISG PFKFB3 can

be induced by viral infection, cytosolic RNA and DNA signals of viral infection, and stimulation of TLRs that use the adaptor TRIF. Further, induction of PFKFB3 in BMDMs requires IFNAR1 and IL-10 signaling, and IL-10 can induce PFKFB3 independently of upstream interferon signaling in differentiated human primary cells.

2.2.2 IFNAR-dependent splicing of PFKFB3 in response to viral infection

Alternative splicing of PFKFB3 and the differential effects of its splice isoforms have been explored in the context of cancer and other disease states (4). However, PFKFB3 splice isoforms have not been characterized in antiviral immune response. We designed qPCR primers to distinguish alternative PFKFB3 exon inclusion: a single forward primer within exon C, one primer spanning the exon C /exon G junction, and one primer spanning the exon C /exon D junction. The regions amplified by the two resultant primer pairs differed by 3 nt in length. We transfected the viral RNA analog poly (I:C) into A549 cells for 8 hours (Figure 2.2 A) and human monocyte-derived macrophages (MDMs, from a single donor, Figure 2.2 B) for 6 hours and quantified relative PFKFB3 exon inclusion by qPCR using the two resultant primer pairs. In both A549 cells and MDMs, the exon C / exon G junction was more abundant than the exon C / exon D junction after poly (I:C) treatment. Then, using MDMs from 3 different patients, we quantified relative PFKFB3 exon inclusion by qPCR after transfection of the viral DNA analog poly (dA:dT) (Figure 2.2 C) or infection with the RNA virus VSV at an MOI of 5.0 (Figure 2.2 D) for 8 hours and found that the exon C / exon G junction was more abundant than the exon C / exon D junction in MDMs after exposure to either viral DNA analog or active RNA viral infection.

Because PFKFB3 can be induced by type I interferon (Figure 2.1 A and B) and because intact type I interferon receptors were required for induction of PFKFB3 in response to either VSV infection or TLR4 stimulation with the bacterial lipopolysaccharide component Lipid A (Figure 2.1 E and F), we asked if interferon signaling also played a role in alternative splicing of PFKFB3. We transfected WT and IFNAR1 KO BMDMs with poly (dA:dT)

(Figure 2.2 E) or infected them with VSV-GFP at an MOI of 5.0 (Figure 2.2 F) for 6 hours and quantified relative PFKFB3 exon inclusion by qPCR, finding that the exon C / exon G junction was also more abundant than the exon C / D junction in BMDMs after exposure to either viral DNA analog or active RNA viral infection and that the preferential induction of the exon C / exon G junction was lost in the IFNAR1 KO BMDMs. Taken together, these findings indicate that PFKFB3 is preferentially spliced in response to viral infection to favor the A-C-G isoform over the A-C-D isoform, and that this splicing event requires intact type I interferon signaling. Interestingly, although the A-C-D isoform is considered to be the “inducible” form due to increased expression in response to hypoxia or inflammatory stimuli, the A-C-G isoform is chosen in response to viral infection.

2.2.3 Antiviral function of PFKFB3 and its splice isoforms

To substantiate the results of the original antiviral screen using VSV-GFP, we first investigated the effect of PFKFB3 overexpression on infection by other RNA viruses using the same methodology. PFKFB3 overexpression significantly decreased infection by Sendai virus (SeV) or Newcastle Disease virus (NDV) (Figure 2.3 A and B). PFKFB3’s kinase activity is much greater (relative to bisphosphatase activity) than PFKFB1, 2, or 4, but these other isozymes are still active kinases, so we asked if the effect of PFKFB3 overexpression was unique to PFKFB3. We transfected 293T cells with PFKFB1, PFKFB3 or vector control and infected with VSV-GFP at an MOI=0.05 for 12 hours before analyzing infection via the relative size of the GFP+ population as measured by flow cytometry. PFKFB3 strongly decreased the number of infected cells, while PFKFB1 had no effect (Figure 2.3 C). We then asked if PFKFB3 kinase activity or nuclear localization of PFKFB3 were necessary for viral inhibition using mutant PFKFB3 constructs in which the catalytic site of the kinase domain (KD) or nuclear localization signal (NLS) had been disrupted by alanine substitution at key residues. The R75A/R76A KD mutation completely eliminated the effect of PFKFB3 overexpression on VSV-GFP infection in 293T cells, while the K274A/K275A NLS mutation had no effect (Figure 2.3 E).

Because cells specifically induced the A-C-G but not A-C-D isoform of PFKFB3 in response to viral infection and viral PAMPs, and because we found that this signal-dependent splicing was regulated by type I interferon signaling, we asked if exon inclusion affected the antiviral function of PFKFB3. Importantly, exon D inclusion leads to a frameshift that causes alternative translation of exon G into an entirely different C terminal peptide sequence. We reasoned that if PFKFB3 exon inclusion did have an effect on its antiviral function, then this effect could be due either to residues “lost” from exon G’s normal translation or “gained” by the inclusion of exon D and resultant frameshift. We therefore created a truncation mutant lacking exon G, termed A-C, to distinguish effects of exon D inclusion from exon G “loss.” We transfected 293T cells with A-C-G, A-C-D and A-C isoforms of PFKFB3 24 hours prior to infection with VSV-GFP at an MOI of 0.05, using GFP as a transfection control and TBK1 as a positive control for viral inhibition. We then determined the viral titer in the supernatant by plaque assay on MDCK cells 24 hours post infection, finding that expression of the A-C-G isoform and A-C mutant both strongly reduced viral titer while the A-C-D isoform did not (Figure 2.3 F).

2.2.4 Investigating mechanisms of PFKFB3 antiviral function

Cells secrete interferons and other cytokines in response to signals of viral infection, conferring antiviral resistance via autocrine or paracrine signaling. We therefore tested the antiviral effect of PFKFB3-conditioned media, infecting untransfected 293T cells with VSV-GFP in the presence of media conditioned by 293T cells transfected with PFKFB3 or vector control, and found that media conditioned by cells overexpressing PFKFB3 conferred resistance to VSV infection (Figure 2.4 A). Centrifugal filtration of conditioned media to concentrate protein components offered a surprising result: the concentrate had no antiviral effect, but the filtrate, containing molecules less than 3 kDa in size, conferred resistance to viral infection. Moreover, heat treating the conditioned media (15 minutes at 90 degrees C) did not change its ability to inhibit VSV infection, and neither pH adjustment nor the addition of lactic acid to unconditioned media could recreate the conditioned media effect

(data not shown.) These findings suggested that the antiviral effect conferred by PFKFB3-conditioned media was most likely due to increased production and/or secretion of one or more small molecules, i.e. peptides or metabolites, so we began investigation of PFKFB3's antiviral function by investigating the effect of PFKFB3 expression on metabolites in cell media.

We first transfected 293T cells with WT or R75A/R76A kinase domain mutant PFKFB3 and extracted metabolites from the 48-hour conditioned cell media for metabolic footprint analysis by LC/MS. Choline use was sharply decreased in cells overexpressing PFKFB3, though apparently independent of kinase activity (Figure 2.4 B). However, phosphocholine levels were elevated in the media of cells overexpressing WT and not kinase mutant PFKFB3 (Figure 2.4 C). Interestingly, choline is an essential media-supplied nutrient that mammalian cells cannot synthesize *de novo*, indicating decreased choline uptake or increased choline secretion in the PFKFB3 overexpression condition. When we analyzed intracellular metabolites in extracts from similarly transfected cells by LC/MS, we found increased intracellular choline in cells overexpressing WT PFKFB3 but not in those overexpressing the kinase mutant (Figure 2.4 D). Intracellular phosphocholine levels were not significantly changed in either condition (data not shown.) Finally, we investigated the effect of alternative exon inclusion on media choline by colorimetric assay, finding that measured choline concentration was much higher in media from cells overexpressing the A-C-G isoform (10.2 μM) than in media from cells overexpressing the A-C-D isoform (2.7 μM) or transfected with the vector control (4.6 μM) (Figure 2.4 E). The concentration of choline in the cell culture media formulation is 21.3 μM .

Because media phosphocholine and intracellular choline levels were both strongly affected by PFKFB3 overexpression and subject to kinase activity or C-terminal peptide sequence, we investigated the effect of choline supplementation on viral infection. Choline is supplied in cell media as choline chloride, at a concentration of 4 $\mu\text{g}/\text{mL}$. We treated 293T cells with increasing concentrations of choline chloride for 24 hours before infection with VSV-GFP and FACS analysis, as previously described, and found that choline supplementation eliminated VSV infection at a concentration 25x that of normal media formulation, prior to uptake by

cells (Figure 2.4 F.)

2.2.5 Effect of PFKFB3 C-terminal peptide sequence on metabolic impact

Our findings with regard to antiviral response, functional antiviral effect and effect on media choline indicated that PFKFB3 splice isoforms might have significantly different effects on cell metabolism. We again overexpressed the A-C-G and A-C-D PFKFB3 isoforms and the A-C mutant along with a GFP vector control in 293T cells, changing the media to glucose-free media supplemented with [U-13C] glucose 24 hours before quenching and metabolite extraction. Analysis of cell metabolite extracts by LC/MS yielded data indicating a pattern of significant changes in metabolite abundance in cells overexpressing the PFKFB3 A-C-G isoform or A-C mutant not present in cells overexpressing the A-C-D isoform.

As expected, PFKFB3 overexpression had a marked effect on glucose use in 293T cells. As shown in Figure 4, PFKFB3 A-C-G and A-C but not A-C-D increased intracellular abundance of the isomeric metabolites glucose 6-phosphate (G6P) and fructose 6-phosphate (F6P), suggesting increased hexokinase activity (Figure 2.5 A). The relative amounts of G6P, F6P and the PFK-1 product fructose 1,6-bisphosphate were much higher in cells overexpressing the A-C mutant than in cells expressing PFKFB3 isoforms (Figures 2.5 A and B). Continuing stepwise through glycolytic intermediates, dihydroxyacetone phosphate (DHAP) was decreased in cells overexpressing the A-C-G isoform or A-C mutant (Figure 2.5 C), though no decrease was evident in its isomer glyceraldehyde 3-phosphate (Figure 2.5 D) However, dramatically decreased abundance in cells overexpressing the A-C-G isoform or A-C mutant but not A-C-D isoform was evident for the subsequent glycolytic intermediates 1,3-bisphosphoglycerate (13BPG), 3-phosphoglycerate (3PG), and phosphoenolpyruvate (PEP); 2-phosphoglycerate (2PG) was not measured (Figures 2.5 E, F, G). All three PFKFB3 isoform or mutant constructs had only mild effects on pyruvate and lactate abundance, though the A-C mutant exhibited a stronger and more significant increase in intracellular lactate (Figures 2.5 H and I).

Our previous observations of increased choline and phosphocholine in the media of cells

overexpressing PFKFB3 suggested increased intracellular abundance might also occur. Intracellular choline was mildly increased in cells overexpressing the PFKFB3 A-C-G isoform or A-C mutant but not those overexpressing the A-C-D isoform (Figure 2.6 A). Choline is incorporated into phosphatidylcholine via a three-step process that begins with phosphorylation by choline kinase in the cytoplasm, followed by attachment of CDP from CTP by choline-phosphate cytidyltransferase in the nucleus. We found that while phosphocholine (P-choline) was strongly decreased by PFKFB3 A-C-G and A-C expression (Figure 2.6 B), the same conditions produced dramatic increases in CDP-choline abundance that could not be explained by changes in CTP (Figures 2.6 C and D). The A-C-D isoform failed to produce this effect on CDP-choline. Though ethanolamine is incorporated into phosphatidylethanolamine in a similar process, in which the same choline-phosphate cytidyltransferase reacts CTP with phosphoethanolamine (P-EtA) to form CDP-ethanolamine (CDP-EtA), the C terminal peptide sequence of PFBF3 did not affect P-EtA as it did P-choline, and increases in CDP-EtA were not significant (Figures 2.6 E and F).

Choline is also converted to betaine, an important methyl donor in the regeneration of methionine from homocysteine. We found a dramatic increase (50-100 fold) in homocysteine abundance in cells overexpressing PFKFB3 A-C-G or A-C but not A-C-D (Figure 2.6 G). The alternative pathway for methionine regeneration from homocysteine uses the methyl donor 5,10-methylene tetrahydrofolate (5,10-mTHF) at the cost of 1) its conversion to 10-formyl THF for use in purine synthesis and 2) the de novo synthesis of dTTP, converting dUMP to dTMP. We observed decreased dTTP abundance in cells overexpressing PFKFB3 A-C-G or the A-C mutant (Figure 2.6 H).

2.2.6 PFKFB3 binds HK2: potential role of PFKFB3 in poly (I:C)-induced hexokinase activity

The full picture of PFKFB3's antiviral activity remains unclear, as the metabolic effects of overexpression, specifically those highlighted by the different effects of alternative splice isoforms, suggest impacts beyond increased glycolytic flux. Although we found that

the nuclear localization signal in exon C was not required for PFKFB3 antiviral activity, the reported activity of PFKFB3 in the nucleus made us wonder if PFKFB3 and its activity might be functionally localized elsewhere in the cell. Further, the alternative exon inclusion we observed in response to viral infection and the lack of antiviral activity in the A-C-D isoform suggested that residues in exon D might interfere with this localization. The PFKFB3-related protein TIGAR was reported to localize to the outer mitochondrial membrane (OMM) under hypoxia, binding and altering the activity of the mitochondrial hexokinase HK2. We observed increased in vitro hexokinase activity in whole cell lysates from 293T after transfection of poly(I:C), a condition under which PFKFB3 expression is increased. Co-localization of glycolytic enzymes to the OMM in enzyme complexes called metabolons has been well documented in plants, and several glycolytic enzymes have been reported to co-localize to the outer membrane of the lysosome in a similar fashion in human cells, including PFKFB3 itself via interaction with the Ragulator protein RagB (3). We therefore considered the possibility that PFKFB3, like TIGAR, might bind the mitochondrial hexokinase HK2, with a guess that exon inclusion might affect this interaction. We overexpressed FLAG-tagged PFKFB3 A-C-G, A-C-D isoforms and the A-C mutant construct with and without co-expression of MYC-tagged HK2, purified HK2 using MYC antibody-conjugated beads and performed Western blot for FLAG and MYC tags in the input and immunoprecipitate. As shown in Figure 2.7, PFKFB3 clearly co-precipitates with HK2. To our knowledge, this is the first report of PFKFB3-HK2 interaction. However, C terminal exon inclusion did not affect HK2 binding in the overexpression condition, and further work is needed to determine what PFKFB3 residues are required for binding to HK2, and whether HK2 binding is required for PFKFB3 antiviral activity. If PFKFB3 binding is involved in its antiviral function, exon inclusion may affect binding to another enzyme or binding partner at the mitochondrial hexokinase-VDAC hub.

2.3 Discussion

2.3.1 Type I interferon signaling mediates preferential induction of the PFKFB3 A-C-G isoform in response to viral infection

PFKFB3 had been identified as an ISG with antiviral functions, but if and how it might be induced in response to viral infection was unclear. Our results establish PFKFB3 induction in response to both viral infection and molecular sensing of viral nucleic acid analogs in murine BMDM, human MDM and the human lung adenocarcinoma A549 cell line. We used IFNAR KO BMDM to show that ablation of type I interferon signaling eliminates PFKFB3 induction in response to viral infection. We were also able to see a marked difference in induction between the A-C-G and A-C-D isoforms of PFKFB3, with little to no change in the expression of the A-C-D isoform in response to viral infection or viral infection signals even as the total population of PFKFB3 mRNA increased. The A-C-G isoform, however, was strongly induced, with induction levels even higher than the total PFKFB3 population. Somewhat counterintuitively, the fold change representation of data is such that the extreme difference between the A-C-G isoform and the total PFKFB3 population seen in A549 cells (Figure 2A) indicates a switch from A-C-D to A-C-G expression in cells already strongly expressing PFKFB3 (see Figure 1D); the unstimulated C_q values were similar between primers. On the other hand, results in which the increase in A-C-G expression is similar in magnitude to the increase in the total population are better characterized as preferential induction of the A-C-G isoform. Excitingly, type I interferon's role in PFKFB3 induction downstream of cytosolic viral nucleotide analog sensing is apparently coupled to the preferential induction of the A-C-G isoform.

2.3.2 IL-10 but not Hif1a potentiates IFNAR-dependent induction of PFKFB3 by TLR4

PFKFB3 is also known to be induced in response to LPS stimulation of TLR4.⁽¹²⁾ Using TRIF KO BMDM, we showed that PFKFB3 induction downstream of membrane

TLR stimulation requires the TLR adaptor molecule TRIF. Hif1a is a transcription factor known to induce PFKFB3 in hypoxic conditions, and we found that Lipid A stimulation of TLR4 increased protein levels of both PFKFB3 and Hif1a in a TRIF-dependent manner. However, poly (I:C) stimulation of TLR3 also increased PFKFB3 protein levels in a TRIF dependent manner without increasing Hif1a levels, and treatment with the Hif1a stabilizer DMOG strongly increased Hif1a expression levels without affecting PFKFB3. The conclusion from this data is that increased Hif1a is neither necessary nor sufficient to increase PFKFB3 protein expression in normoxic BMDM.

Ip et al previously found that the extracellular acidification rate, a measure of glycolytic flux, was increased and the oxygen consumption rate, a measure of oxidative phosphorylation, was decreased in LPS-stimulated IL-10 KO BMDM and that IL-10 treatment decreased glycolytic flux(13). We found that loss of IL-10 in BMDM also led to a defect in PFKFB3 induction after Lipid A stimulation, indicating that PFKFB3 is not likely to be the target of IL-10's glycolytic inhibition. Our analysis of publicly available data for MDM treated with IL-10 supports this unlikelihood, given the increase in PFKFB3 expression after IL-10 treatment. It also suggests that hexokinase is a more likely point of glycolytic control for IL-10, as the cytoplasmic HK3 isozyme was upregulated and the mitochondrial HK2 enzyme downregulated in that dataset. Nevertheless, accepting a role for IL-10 in the induction of PFKFB3, an enzyme with the potential to increase glycolytic flux, might require a looser grip on a M1/M2 macrophage-based concept of metabolism and inflammation or an expanded view of PFKFB3 function.

2.3.3 Antiviral function of PFKFB3

Our results indicate that The A-C-G isoform of PFKFB3 functions as an antiviral ISG, limiting infection by VSV (vesicular stomatitis virus, now known as Indiana vesiculovirus), Sendai virus (now known as murine respirovirus) and Newcastle disease virus and exerting antiviral function via activity of its kinase domain. We also found that PFKFB1, an isozyme with reasonably high kinase activity, did not exert antiviral function like PFKFB3, suggesting

that PFKFB3's antiviral function might be due to both its kinase activity and some other as yet unidentified activity in the cell. We originally thought that the C terminal peptide sequence encoded by Exon G (and undisturbed by Exon D-induced frameshift) might impart antiviral function to PFKFB3, but our use of the A-C mutant, which behaved similarly to A-C-G in the infection experiments and later metabolic experiments, indicated that the loss of Exon G did not lead to loss of antiviral function; instead, inclusion of exon D in PFKFB3 mRNA restricted function, ostensibly via effects on residues outside either exon G or D.

This study is limited in that we have only investigated the antiviral function of PFKFB3 against enveloped RNA viruses, so that we don't know whether or not PFKFB3 has any kind of broadly inhibiting antiviral function. However, we have seen that PFKFB3 is induced in response to viral RNA and DNA signals both, and for RNA saw induction via cytosolic or extracellular routes of encounter. Further experiments are needed to investigate the breadth of PFKFB3's antiviral effect.

2.3.4 Choline or related metabolites may confer antiviral function in PFKFB3-conditioned media

Using PFKFB3-conditioned media separated into ≤ 3 kDa and ≥ 3 kDa fractions by protein concentrator spin column, we found that the antiviral factor in PFKFB3-conditioned media must be ≤ 3 kDa. Though we went ahead with the hypothesis that PFKFB3 overexpression led to increased media concentration of a small molecule metabolite, it remains possible that PFKFB3 overexpression actually (or, also) leads to secretion of an antiviral peptide. Our analysis of PFKFB3's metabolic footprint indicated strong changes in choline use and the level of extracellular phosphocholine, and we could also see increased intracellular choline and increased media choline (which we think of as unused choline) by kinase assay. Choline is supplemented in mammalian cell culture media because mammalian cells cannot synthesize it *de novo*, so the finding that PFKB3 decreases net choline uptake from cell media was surprising given increased uptake of glucose and glutamine (not shown.) In an example of opposite effect, HDAC inhibition was reported to inhibit proliferation by

increasing choline uptake and incorporation into phosphatidylcholine in MCF7 cells via increased expression of the choline transporter SLC44A1, choline kinase A and phospholipase (14). Nevertheless, choline addition to media of cells just prior to infection with VSV-GFP decreased infection in a dose-dependent manner. Unfortunately none of these results indicate that choline is actually the causative agent in PFKFB3's antiviral effect; answering that question will require systematic investigation of PFKFB3's potential effects on choline metabolism pathway component enzymes.

2.3.5 PFKFB3 A-C-G increases intracellular abundance of upper glycolysis reaction products

We saw a marked difference in the effect of PFKFB3 A-C-G expression on the products of upper and lower glycolysis (demarcated by the line between formation of F16BP and its downstream product.) Recently, a systems-level analysis of genes controlling glycolytic flux identified glucose import, hexokinase activity, phosphofructokinase activity, and lactate export as the four meaningful points of glycolytic flux control, further finding that the steps of lower glycolysis (after creation of F16BP) did not meaningfully influence glycolytic flux, and that increased F16P pool was a major flux signature (15). This description fits the metabolomic profile of PFKFB3 A-C-G and A-C perfectly, indicating that as expected PFKFB3 increased glycolytic flux. Glycolytic intermediates are also part of other metabolic pathways. The intermediate 3PG for instance, the pool of which was reduced by PFKFB3 A-C-G or A-C, is converted to serine by PHGDH to be incorporated into phospholipids or enter the folate cycle of one carbon metabolism. Later steps of PFKFB3 might have reduced metabolite pools not because of lesser contribution to glycolytic flux but because (or also because) those pools are being rapidly depleted to meet other cellular needs.

2.3.6 PFKFB3 A-C-G breaks choline and one-carbon metabolism

Overexpression of PFKFB3 A-C-G or A-C both strongly increased intracellular CDP-choline levels. Choline has two fates in the cell: incorporation into the head group of the

phospholipid membrane component phosphatidylcholine (PC) or mitochondrial conversion to betaine, an intermediate of one carbon metabolism at the junction of folate and methionine cycles. One carbon metabolism controls the availability of methyl donors for purine and dTMP synthesis and the transmethylation of proteins, DNA, lipids and phospholipids. Choline-derived betaine (trimethylglycine) donates its methyl group to regenerate methionine from homocysteine and become dimethylglycine (DMG), a glycine and serine precursor. Methionine can also be regenerated from homocysteine by 5-methyl tetrahydrofolate (5-mTHF) in a vitamin B12-dependent reaction, but this pathway comes at a cost to the essential use of the 5-mTHF precursor 5,10-mTHF for thymidylate synthase conversion of dUMP to dTMP in the de novo synthesis of dTTP. In the absence of this 5,10-mTHF –facilitated de novo synthesis activity, cells must salvage existing thymidine for nucleic acid biosynthesis using thymidine kinase. Neither pathway of methionine regeneration seems to have been working in cells overexpressing PFKFB3 A-C-G or A-C: the most dramatic effect of PFKFB3 overexpression on metabolite pools was the nearly 100-fold increase in intracellular homocysteine. This accumulation is strongly indicative of inhibition in the linked folate and methionine cycles of one-carbon metabolism, which are also supported by serine and choline input.

In medicine, hyperhomocysteinemia (HHCys) is the condition of elevated serum homocysteine. HHCys is a biomarker for cardiovascular disease and a risk factor for other age and/or diet-related diseases including dementia, Alzheimer’s disease, hepatic steatosis, and colorectal cancer (*16, 17*). In a tissue context, homocysteine treatment caused mitochondrial dysfunction leading to ROS generation in rat ischemic brain (*18*). In macrophages, the ultimate effects of elevated homocysteine are less clear: homocysteine elicits an M1 (pro-inflammatory) activated phenotype accompanied by increased ROS generation (*19*), yet PFKFB3, considered to be pro-inflammatory in glycolytic effect (*12*), also potentiated suppression of M1 activation by the bacterially-produced dietary component indole (*20*).

2.3.7 Beyond PFK-2 activity: PFKFB3 binds HK2

PFKFB3 bound to and co-precipitated with HK2 *in vitro*, indicating direct protein-protein interaction. To our knowledge this is the first report of PFKFB3/HK2 interaction, but it puts PFKFB3 in good company: PFKFB2 binds the liver hexokinase glucokinase (21) and the fructose 2,6-bisphosphatase TIGAR binds HK2 under hypoxic conditions (22). In addition, Zhang et al recently showed that MAVS interacts with HK2 (23). The C-terminal peptide sequence of PFKFB3 is preferentially chosen, so we thought that PFKFB3 isoforms might vary in their ability to bind HK2. However this interaction did not appear to be affected by the C terminal peptide sequence, as the PFKFB3 A-C-G and A-C-D as well as the A-C mutant form all bound HK2. This result certainly excludes PFKFB3/HK2 interaction from being the sole cause of PFKFB3's antiviral function or metabolic impact, but it may still be involved in these activities. Clearly multiple proteins can interact with HK2, and many more are known to interact with VDAC, the mitochondrial pore with which HK2 is associated, indicating the possibility of more complicated and potentially transient interactions between various components of macromolecular OMM complexes. It would be interesting to see if PFKFB3 can bind hexokinase 3, which like PFKFB3 is induced by both type I interferon and IL-10 treatment. Either way, interaction with HK2 adds a new mitochondrial OMM localization to PFKFB3's growing list; PFKFB3 interacts with cyclin-dependent kinases in the nucleus and (2) and with PFK-1 and Ragulator proteins at the lysosome.(3).

2.3.8 Conclusions

PFKFB3 is a type I interferon-dependent ISG induced in response to viral infection or to viral nucleic acid analogs via type I inteferon signaling that inhibits viral infection via activity of tis kinase domain and in a manner conferrable via its conditioned cell media. In a parallel story, PFKFB3 is an alternatively spliced metabolic regulator with an isoform, A-C-G, that is preferentially induced over another isoform, A-C-D, in the type-I interferon-driven response to viral infection. The apparent dependency of PFKFB3's antiviral and metabolic effects on

the *absence* of the peptide sequence resulting from exon D inclusion suggests that exon D disables PFKFB3 functions and that PFKFB3 function may be modified by localization or interaction mediated by residues in exon D's resultant sequence.

2.4 Methods

2.4.1 Cell culture

HEK 293T and A549 cells were obtained from ATCC. 293T, A549 and BMDM were all cultured in standard conditions using high-glucose Dulbecco's modified Eagle medium (DMEM) formulated with glutamine, without sodium pyruvate and with the addition of 10% fetal bovine serum (FBS) and 1% penicillin/streptomycin (P/S). MDM were cultured in RPMI 1640 medium with the addition of 10% fetal bovine serum (FBS) and 1% penicillin/streptomycin (P/S). FBS was heat-inactivated (30 min at 55 C) before use in MDM and BMDM cultures.

2.4.2 Peripheral Human monocyte-derived macrophages

Mononuclear cells were harvested from the peripheral blood of healthy human donors (UCLA Institutional Review Board No. 92-10-591-31) and adherent monocytes were isolated as previously described before differentiation into macrophages by culture in the presence of M-CSF (500 U/ml) for 7 days (24).

2.4.3 Murine bone marrow-derived macrophages

Bone marrow was harvested from the femurs and tibia of 8-12 week male C57Bl6 mice (WT, IFNAR KO, TRIF KO, IL-10 KO), passed through a 45 micron filter, resuspended in cold ACK lysis buffer for 30 seconds, and resuspended in DMEM + 10% FBS for cell counting. Cells were seeded at 500,000 cells/well of a 6 well plate and cultured in the presence of L929 supernatant containing titered M-CSF for 7 days. Non-adherent cells were removed at 5 days.

2.4.4 Coimmunoprecipitation

Whole cell lysates in passive lysis buffer were incubated with anti-c-Myc agarose (Pierce™ 20168) overnight at 4 C before washing with RIPA buffer and elution by boiling in SDS loading buffer containing stabilized reducing agent.

2.4.5 Western blot

Cells were lysed in RIPA buffer containing protease inhibitor cocktail and insoluble material was precipitated by centrifugation. Lysates were boiled in SDS sample loading buffer with BME. Proteins were separated in 10% bis:tris acrylamide gels by 100V current applied to running buffer. Gels were washed and proteins were transferred to low-fluorescence Immobilon-LF PVDF membranes (Millipore) by current applied to running buffer containing 10% methanol. Membranes were blocked in SEA BLOCK blocking buffer (Thermo Fisher) and incubated with primary antibodies in PBS + 0.01% Tween-20 overnight at 4 C. After sufficient washing in PBST, membranes were incubated with fluorescent-conjugated secondary antibodies for 1 hour at room temperature, washed again and scanned using the Odyssey system (Li-Cor).

2.4.6 qPCR analysis of gene expression

Cells were infected with VSV-GFP at MOI=5 or transfected with poly (I:C) or poly (dA:dT) complexed with Lipofectmine 2000 in OMEM 6 hours before RNA extraction with TriZol (Invitrogen) and cDNA generation with the iScript synthesis kit (Bio-Rad), following manufacturer's protocols. qPCR reactions were prepared with 10mM primers in iTaq SYBR green master mix and run for 40 cycles in a CFX96 real-time PCR system (BioRad). Fold changes were calculated using the standard $\Delta\Delta C_q$ method with human or mouse L32 as internal control. Primer sequences are listed in Table 2.1

2.4.7 PFKFB3 plasmid constructs

Human PFKFB3 in the pM02 entry vector was obtained from Genecopoeia as part of a custom screening panel and double point mutations R75A/R76A or K274A/K275A were made by site-directed mutagenesis using KOD HotStart polymerase and the In-Fusion HD cloning system. GFP and rLuc controls were in the same pM02 vector. Mouse PFKFB3 (MR227632), PFKFB1 (MR218288) and HK2 (MR211170) in the pCMV6 entry vector were obtained from Origene and the A-D-G isoform and A-C mutant was generated by inverse PCR using KOD HotStart polymerase and the In-Fusion HD cloning system. PFKFB3 constructs and HK2 were transferred to single N-terminal tagged destination vectors from Origene (pCMV6-AN-DDK, pCMV6-AN-MYC) via their PrecisionShuttle kit for use in coimmunoprecipitation experiments.

2.4.8 Viral infections, flow cytometry and plaque assay

293T cells were infected with VSV-GFP at at MOI of 0.05 or 0.1 for 12 hours, and SeV-GFP or NDV-GFP at an MOI of 1 for 24 hours prior to fixation for analysis of GFP⁺ by flow cytometry. For SeV and NDV, media containing virus was removed and replaced with fresh media 1 hour after infection. Flow data was analyzed with BD Biosciences FACSuite and/or FlowJo software. For the plaque assay, 293T cells were infected with VSV-GFP and 24 hours later supernatant dilutions were used to inoculate MDCK cells seeded at 1e6 cells/well of a 6 well semi-soft agarose coated plate, washed after 1 hour and incubated for 2 days before removal of media and plaque staining with 0.3% crystal violet. Plaques counts for each dilution were used to calculate viral titer as plaque-forming units (PFU).

2.4.9 Metabolite extraction

For metabolic footprinting 10 uL of cell media was added to 500 uL 80% methanol. Methanol was evaporated under vacuum and metabolites re-suspended in 70% acetonitrile. For cell extracts, cells were washed in 150 mM cold ammonium acetate (pH 7.3) before quenching with 500 uL 80% methanol kept at -80 C. Cells were scraped in methanol and 10

nM D/L norvaline was added to the suspensions as an internal standard. Insoluble material was precipitated by centrifugation and washed with an additional 500 μ L 80% methanol, and the supernatants containing metabolites were combined. Methanol was evaporated under vacuum from all samples and metabolites re-suspended in 70% acetonitrile.

2.4.10 Ultra-High Performance Liquid Chromatography Mass Spectrometry (UPLC-MS)

For the mass spectrometry-based analysis of the sample, which was performed by the UCLA metabolomics core, 5 μ L were injected onto a Luna NH2 (150 mm \times 2 mm, Phenomenex) column. The samples were analyzed with an UltiMate 3000RSLC (Thermo Scientific) coupled to a Q Exactive mass spectrometer (Thermo Scientific). The Q Exactive was run with polarity switching (+3.50 kV/-3.50 kV) in full scan mode with an m/z range of 65-975. Separation was achieved using A) 5 mM NH₄AcO (pH 9.9) and B) ACN. The gradient started with 15% A) going to 90% A) over 18 min, followed by an isocratic step for 9 min and reversal to the initial 15% A) for 7 min. Metabolites were quantified with El Maven (v0.2.4) using accurate mass measurements (≤ 3 ppm) and retention times of pure standards. Data analysis was performed using the statistical language R. For the PCA and clustering analyses, only metabolites with an ANOVA p-value ≤ 0.05 were incorporated. For visualization using heatmaps, metabolites were scaled across samples but not across metabolites. To assess what metabolites contributed the most to a given metabolic phenotype, we calculated the correlation between the loading vector for a given metabolite and the score vector of a given sample for PCs 1 and 2.

2.4.11 Choline assay

Media choline concentration was measured via fluorimetric assay using the choline standards and reaction mix in the Amplate Choline Quantitation Kit (AAT Bioquest 40007) and a plate reader set for Ex/Em=530 nm/590 nm per kit instructions. Choline concentration

was normalized to total protein in the sample measured via BCA assay.

Table 2.1: qPCR primer list

Mouse	Forward	Reverse
L32	5'-CACCAGTCAGACCGATATGTGA-3'	5'-ATCAGGATCTGGCCCTTGAACC-3'
PFKFB3 (all)	5'-CATCTGTCACCAGGCTGTTCT-3'	5'-GTGGAGCGGACATTTTCAGGTA-3'
C-D junction	5'-AACAGCTTTGAGGAGCGTGT-3'	5'-TCCCTAGCAAAGGTTGTCCG-3'
C-G junction	5'-CAACAGCTTTGAGGAGCGTG-3'	5'-GGAGCTCTTCATGTTTTGTCCG-3'
Human	Forward	Reverse
L32	5'-CGTCCCTTCTCTCTTCCTCGG-3'	5'-ACATATCGGTCTGACTGGTGC-3'
PFKFB3 (all)	5'-CTGCTTGCCTACTTCCTGGATA-3'	5'-GCGTCAGTTTCAGGACGGTG-3'
C-D junction	5'-CCACCAAAAAGCCTCGCATC-3'	5'-GCCCTAGCAAAGGTTGTCCA-3'
C-G junction	5'-CCACCAAAAAGCCTCGCATC-3'	5'-GGGAGCCTTTCATGTTTTGTCC-3'

2.5 Figure Legends

2.5.1 The type I-specific ISG PFKFB3 is induced in response to viral infection by cytosolic and Toll-like receptors, type I interferon signaling and the cytokine IL-10.

(A) Microarray relative expression profile of the four mammalian phosphofructokinase-2/fructose 2,6-bisphosphatase (PFK-2/FBPase) genes in murine bone-marrow macrophages (BMDM) 2.5 hours after treatment with IFN α (62 U/mL) or IFN γ (1 U/mL). (B) RNAseq relative expression profile of PFKFB3 in human monocyte-derived macrophages (MDM) 2, 6, or 24 hours after treatment with IFN β (285 U/mL) or IFN γ (1.5 ng/mL). (C) qPCR analysis of fold change in PFKFB3 mRNA expression, relative to respective uninfected controls, in WT and IFNAR KO BMDM 6 hours after VSV-GFP infection at multiplicity of infection (MOI) of 5. (D) Western blot for protein levels of PFKFB3 and beta actin in A549 whole cell lysates (WCL) 18 hours after transfection delivery of poly (I:C) or poly (dA:dT). (E) Western blot for protein levels of PFKFB3, Hif1a and beta actin in WCL of WT or TRIF KO BMDM 16 hours after media addition of DMOG, Lipid A (100 ng/ml), poly (I:C), or Pam3CSK4. (F) qPCR analysis of fold change in PFKFB3 mRNA expression, relative to respective untreated controls, in WT, IFNAR KO and IL10 KO BMDM 6 hours after treatment with Lipid A (100 ng/ml). (G) Microarray relative expression profile of PFKFB3-related genes in human peripheral blood mononuclear cells (PBMC) 24 hours after treatment with IL-10 (10 ng/mL).

2.5.2 Type I interferon-dependent alternative splicing of PFKFB3 in innate antiviral response.

qPCR analysis of fold change in mRNA expression of PFKFB3 and the C-D and C-G PFKFB3 exon junctions in A549 cells 8 hours after poly (I:C) transfection (A), single donor MDM 6 hours after poly (I:C) transfection (B), multiple donor MDM 8 hours after poly (dA:dT) transfection (C) or vesicular stomatitis virus (VSV) infection at MOI=5 (D), and

in WT and IFNAR KO BMDM 8 hours after poly (dA:dT) transfection (E) or vesicular stomatitis virus (VSV) infection at MOI=5 (F).

2.5.3 PFKFB3 inhibits viral infection dependent on kinase activity and C terminal peptide sequence.

(A and B) Flow cytometry analysis of GFP⁺ population mean fluorescence intensity (MFI) in 293T cells transfected with PFKFB3 or vector control 24 hours prior to infection with GFP-tagged Sendai virus (SeV-GFP, A) or Newcastle disease virus (NDV-GFP, B) at MOI=1. Media was replaced 1 hour after infection and cells were fixed at 24 hours. (C) Flow cytometry analysis of GFP⁺ proportion in 293T cells transfected with plasmids expressing WT PFKFB3, PFKFB3 R75A/R76A kinase domain mutant, or PFKFB3 K274A/K275A NLS mutant and a vector control 24 hours prior to infection with GFP-tagged vesicular stomatitis virus (VSV-GFP, MOI=0.1) for 12 hours. (D) Diagram of mutant constructs. X denotes approximate location of mutated residues for R75A/R76A kinase mutant and K274/K275 NLS mutant, while the region after exon C is shown missing for the A-C terminal exon deletion mutant. (E) Flow cytometry analysis of relative GFP⁺ proportion in 293T cells transfected with plasmids expressing PFKFB1 or PFKFB3 and a vector control 24 hours prior to infection with VSV-GFP at MOI=0.1 for 12 hours. (F) Viral titer (determined by plaque assay on MDCK cells) in supernatant of 293T cells transfected with plasmids expressing A-C-G, A-C-D and A-C isoforms of PFKFB3 24 hours prior to infection with VSV-GFP at MOI=0.01 for 24 hours.

2.5.4 PFKFB3-conditioned media confers antiviral effect and PFKFB3 alters metabolic footprint in media.

(A) Flow cytometry analysis of relative GFP⁺ proportion in 293T cells transfected with PFKFB3 or vector control and 293T cells treated with over 3 kDa concentrate (Top) or below 3 kDa filtrate fractions of media conditioned by 293T cells transfected with PFKFB3 or vector control. (B and C) Relative difference versus unused cell culture media of choline

(B) and phosphocholine (C) abundance in media extracts from 293T cells at 48 hours after transfection with WT PFKFB3, the PFKFB3 R75A/R76A kinase mutant or GFP control. (D) Relative abundance of choline in metabolite extracts from 293T cells 48 hours after transfection with plasmids expressing PFKFB3 A-C-G, A-C-D or vector control, analyzed by LC/MS and normalized to vector control. (E) Concentration of choline assayed in the media of cells overexpressing PFKFB3 A-C-G, A-C-D or vector control. (F) 293T cells were treated with increasing doses of choline chloride prior to infection with VSV-GFP and GFP+ cells were counted by flow cytometry. Infection is indicated as the GFP+ percentage of total cell number.

2.5.5 Effects of PFKFB3 C-terminal peptide sequence on glycolytic metabolites.

Relative abundance of the glycolytic intermediate metabolites glucose 6-phosphate/fructose 6-phosphate (G6P/F6P, isomers not distinguished, A), fructose 1,6-bisphosphate (F16BP, B), dihydroxyacetone phosphate (DHAP, C), glyceraldehyde 3-phosphate (G3P, D), 1,3-bisphosphoglycerate (13BPG, E), 3-phosphoglycerate (3PG, F), and phosphoenolpyruvate (PEP, G) and the glycolytic products pyruvate (H) and lactate (I) in whole-cell extracts of 293T cells 48 hours after transfection with plasmids expressing A-C-G, A-C-D or mutant A-C forms of PFKFB3, as analyzed by LC/MS and normalized to vector control. The glycolytic intermediate 2-phosphoglycerate (2PG) was not measured.

2.5.6 Effects of PFKFB3 C-terminal peptide sequence on choline-related metabolites.

Relative abundance of choline (A) and the Kennedy phosphatidylcholine synthesis pathway intermediates phosphocholine (P-choline, B) and CDP-choline (C); the CDP source CTP (D) and the Kennedy phosphatidylethanolamine synthesis pathway intermediates phosphoethanolamine (P-EtA, E) and CDP-ethanolamine (CDP-EtA, F); the methionine cycle intermediate homocysteine (G) and dTTP (H) in whole-cell extracts of HEK-293T cells

transfected with A-C-G, A-C-D or mutant A-C forms of PFKFB3, as measured by LC/MS and normalized to vector control. Ethanolamine was not measured.

2.5.7 Co-immunoprecipitation of PFKFB3 isoforms with HK2.

Whole cell lysates from cells overexpressing FLAG-tagged PFKFB3 isoforms and/or MYC-tagged HK2 were incubated with MYC antibody-conjugated beads overnight before repeated washing and subsequent elution of bound protein by boiling in loading buffer. Immunoprecipitated samples and corresponding input lysates were used for Western blot with antibodies against MYC and FLAG tags and against beta actin as a loading control.

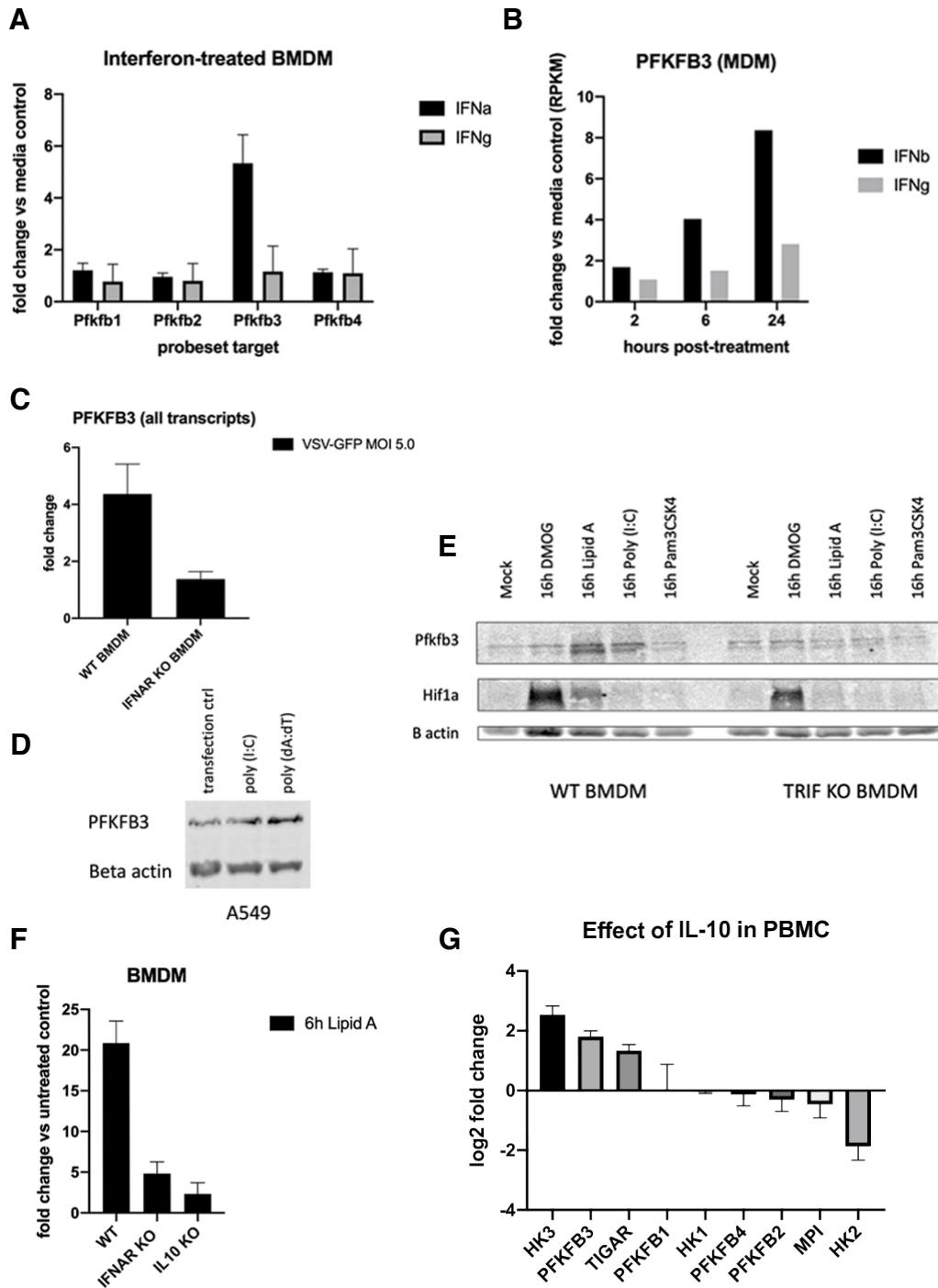


Figure 2.1: PFKFB3 is induced in response to viral infection by cytosolic and Toll-like receptors, type I interferon signaling and the cytokine IL-10.

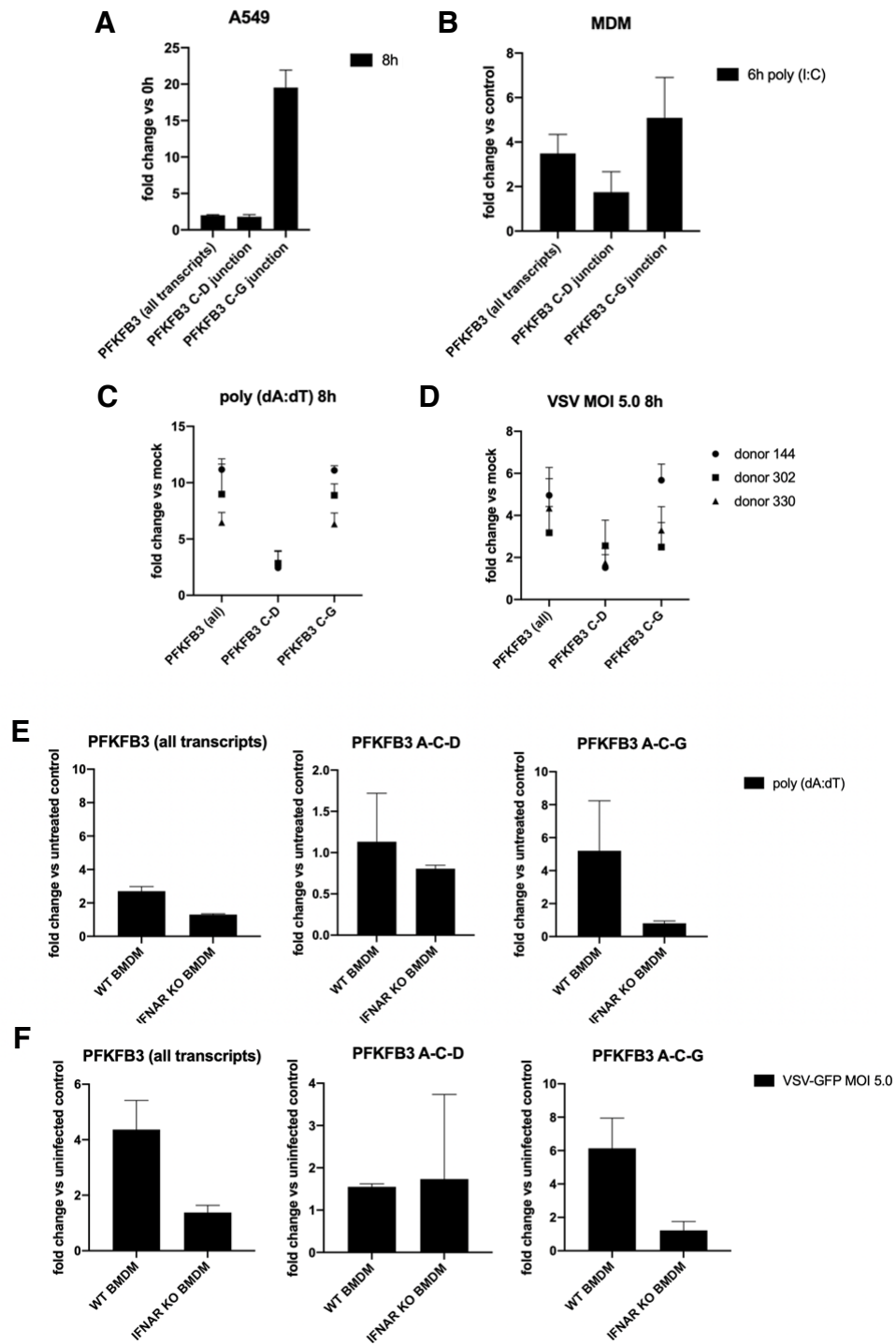


Figure 2.2: Type I interferon-dependent alternative splicing of PFKFB3 in innate antiviral response.

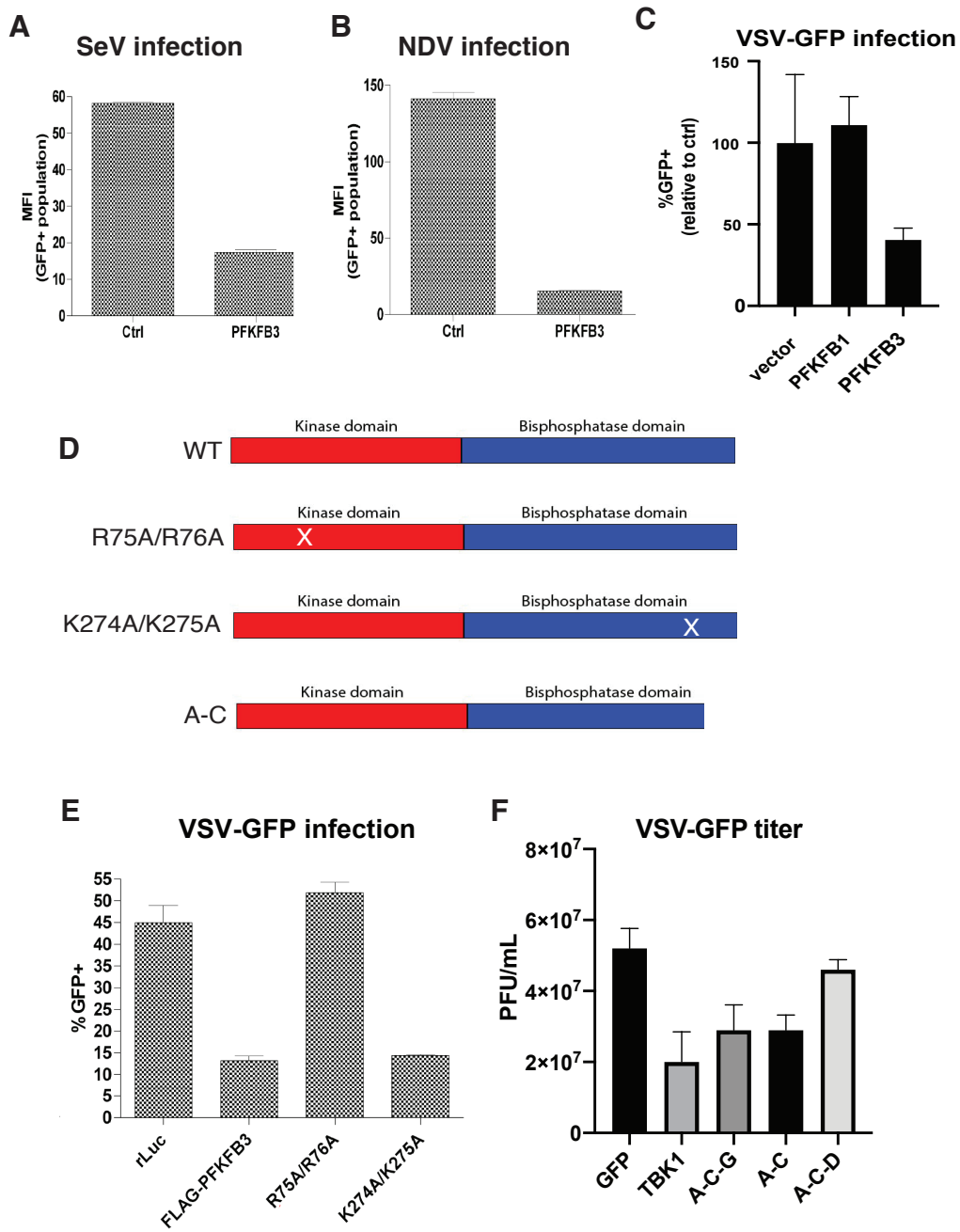


Figure 2.3: PFKFB3 inhibits viral infection dependent on kinase activity and C terminal peptide sequence.

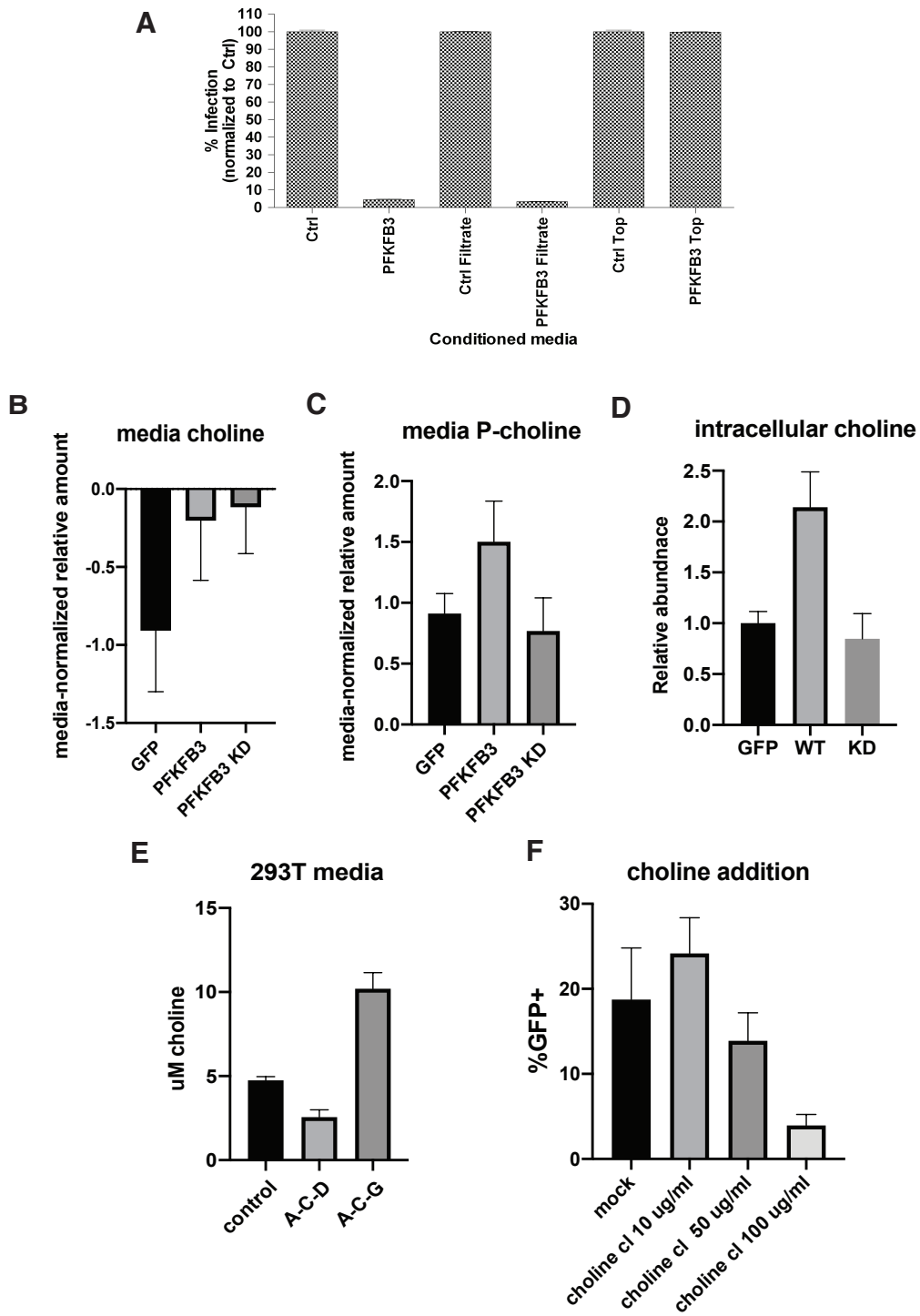


Figure 2.4: PFKFB3-conditioned media confers antiviral effect: possible role for choline.

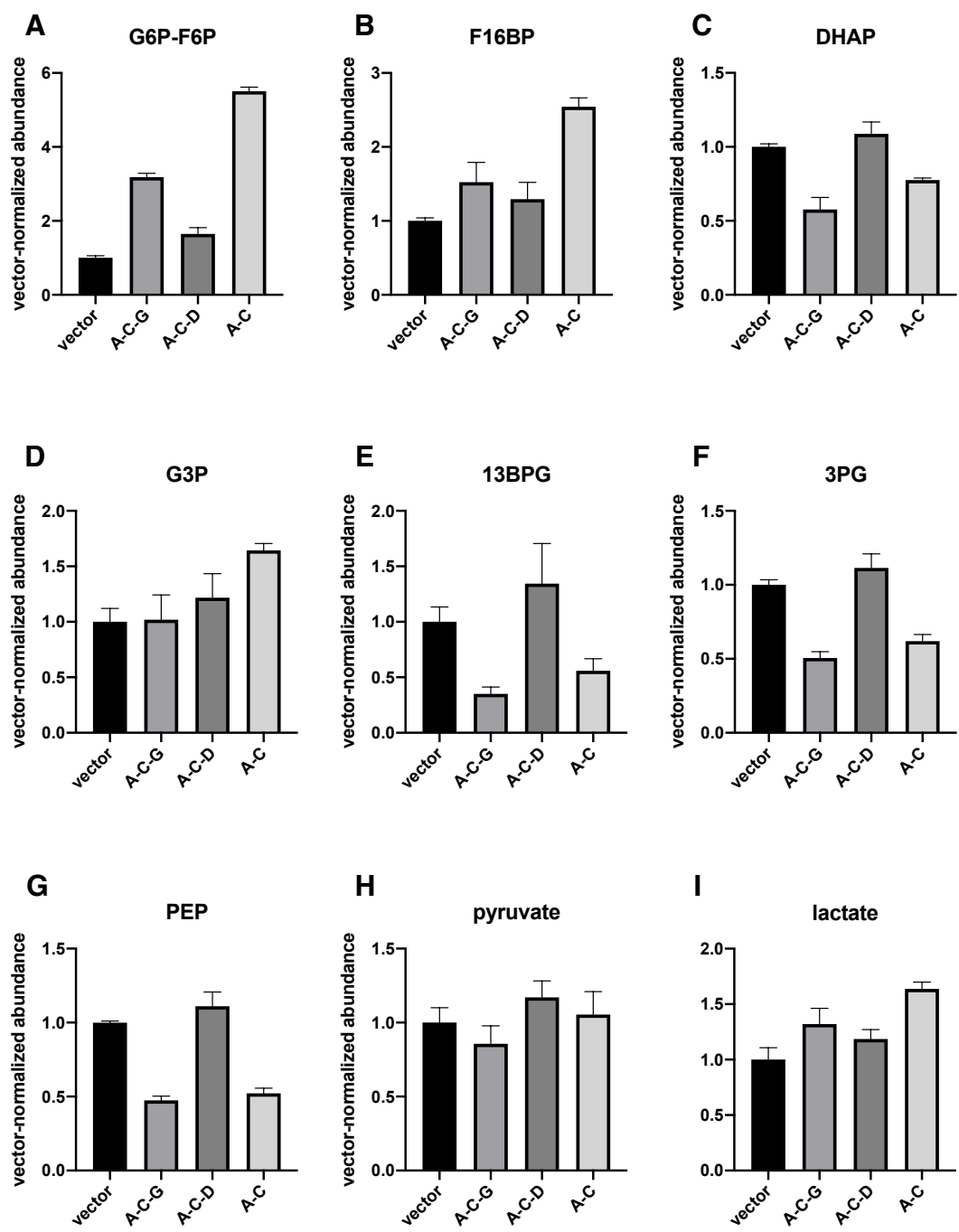


Figure 2.5: Effects of PFKFB3 C terminal peptide sequence on glycolytic metabolites.

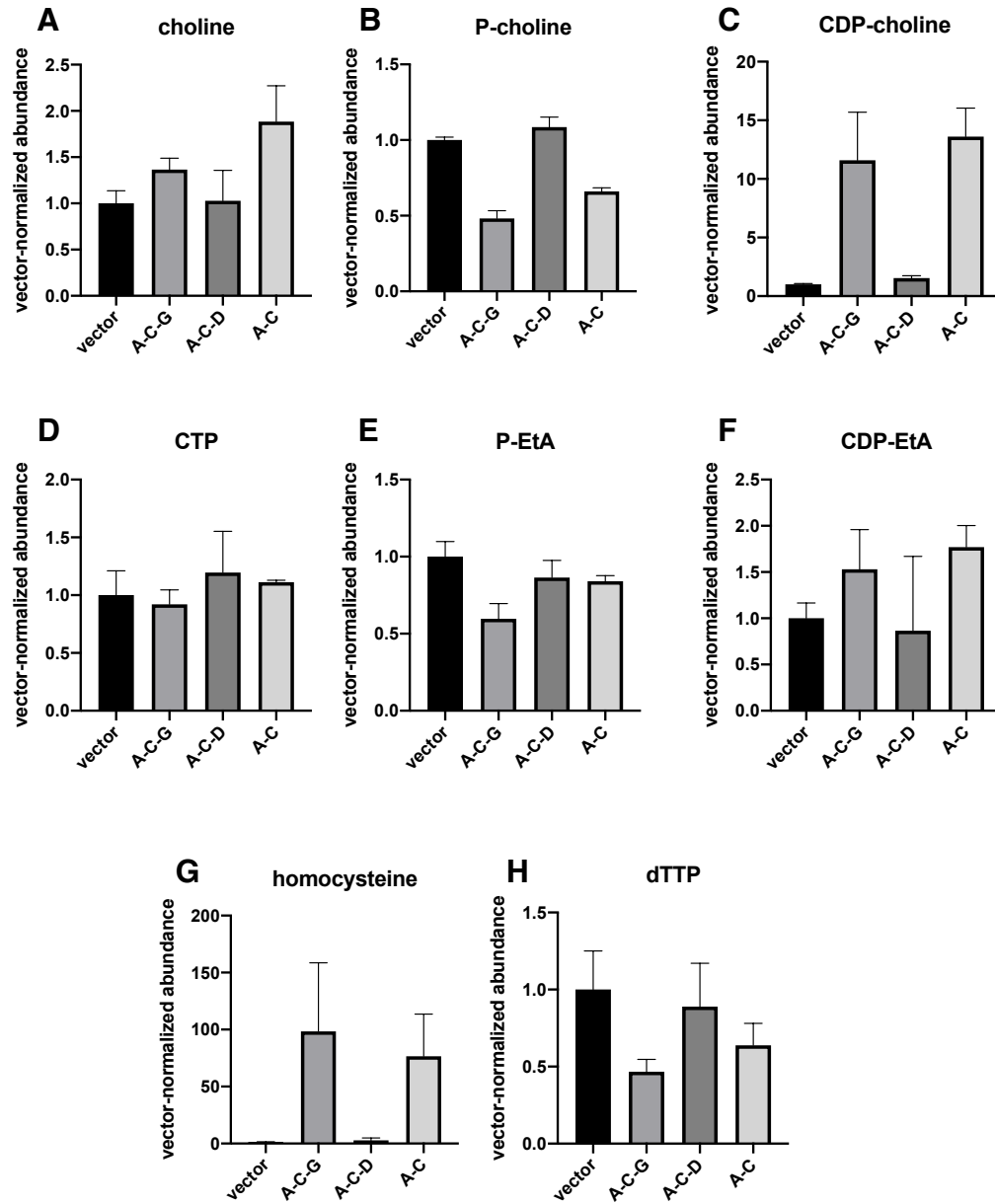


Figure 2.6: Effects of PFKFB3 C terminal peptide sequence on choline-related metabolites.

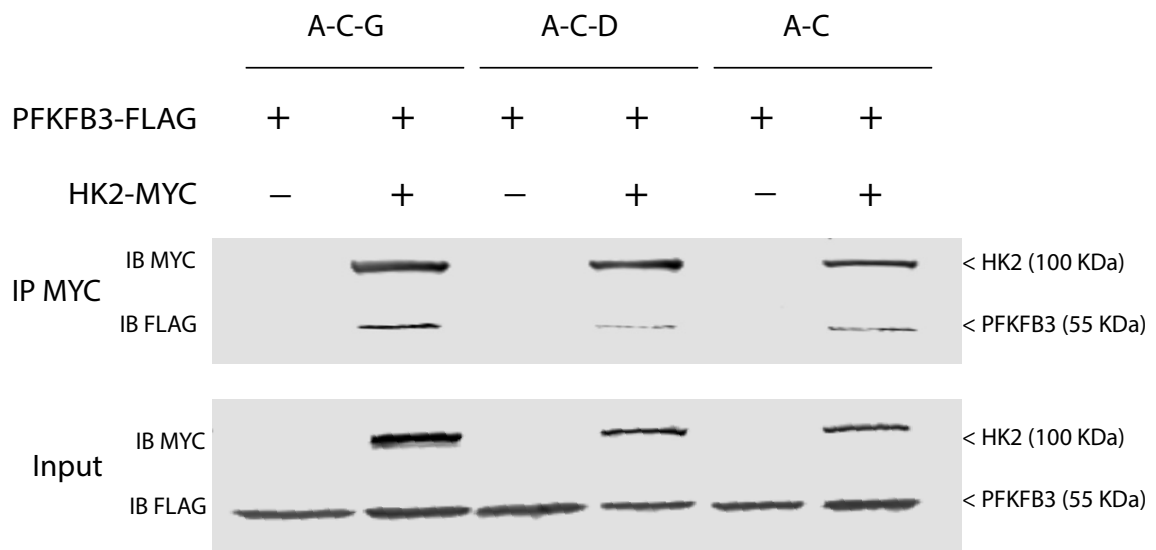


Figure 2.7: Co-immunoprecipitation of PFKFB3 isoforms with HK2.

REFERENCES

1. Clark, J. Enzyme kinetics : 6-phosphofructo-2-kinase/2,6-bisphosphatase. (2014).
2. Yalcin, A. *et al.* 6-Phosphofructo-2-kinase (PFKFB3) promotes cell cycle progression and suppresses apoptosis via Cdk1-mediated phosphorylation of p27. English. *Cell Death & Disease* **5**, e1337 (2014).
3. Almacellas, E. *et al.* PHOSPHOFRUCTOKINASES AXIS CONTROLS GLUCOSE-DEPENDENT mTORC1 ACTIVATION DRIVEN BY E2F1. *iScience* **20**, 434–448. ISSN: 2589-0042 (2019).
4. Bartrons, R. *et al.* Fructose 2,6-Bisphosphate in Cancer Cell Metabolism. *Frontiers in Oncology* **8**, 331. ISSN: 2234-943X (2018).
5. Jiang, H. *et al.* PFKFB3-Driven Macrophage Glycolytic Metabolism Is a Crucial Component of Innate Antiviral Defense. *The Journal of Immunology* **197**, 2880–2890. ISSN: 0022-1767 (2016).
6. Chesney, J. *et al.* Targeted disruption of inducible 6-phosphofructo-2-kinase results in embryonic lethality. English. *Biochemical and Biophysical Research Communications* **331**, 139–146 (2005).
7. Liu, S.-Y., Sanchez, D. J., Aliyari, R., Lu, S. & Cheng, G. Systematic identification of type I and type II interferon-induced antiviral factors. *Proceedings of the National Academy of Sciences* **109**, 4239–4244. ISSN: 0027-8424 (2012).
8. Realegeno, S. *et al.* S100A12 Is Part of the Antimicrobial Network against *Mycobacterium leprae* in Human Macrophages. *PLOS Pathogens* **12**, e1005705. ISSN: 1553-7366 (2016).
9. Barrett, T. *et al.* NCBI GEO: archive for functional genomics data sets—update. *Nucleic Acids Research* **41**, D991–D995. ISSN: 0305-1048 (2013).
10. Iyer, S. S. & Cheng, G. Role of interleukin 10 transcriptional regulation in inflammation and autoimmune disease. English. *Critical reviews in immunology* **32**, 23–63 (2012).

11. Teles, R. M. B. *et al.* Type I Interferon Suppresses Type II Interferon–Triggered Human Anti-Mycobacterial Responses. *Science* **339**, 1448–1453. ISSN: 0036-8075 (2013).
12. Ruiz-Garcia, A. *et al.* Cooperation of Adenosine with Macrophage Toll-4 Receptor Agonists Leads to Increased Glycolytic Flux through the Enhanced Expression of PFKFB3 Gene. English. *The Journal of biological chemistry* **286**, 19247–19258 (2011).
13. Ip, W. K. E., Hoshi, N., Shouval, D. S., Snapper, S. & Medzhitov, R. Anti-inflammatory effect of IL-10 mediated by metabolic reprogramming of macrophages. *Science* **356**, 513–519. ISSN: 0036-8075 (2017).
14. Ward, C. S., Eriksson, P., Izquierdo-Garcia, J. L., Brandes, A. H. & Ronen, S. M. HDAC Inhibition Induces Increased Choline Uptake and Elevated Phosphocholine Levels in MCF7 Breast Cancer Cells. *PLoS ONE* **8**, e62610 (2013).
15. Tanner, L. B. *et al.* Four Key Steps Control Glycolytic Flux in Mammalian Cells. *Cell Systems* **7**, 49–62.e8. ISSN: 2405-4712 (2018).
16. McCully, K. S. Hyperhomocysteinemia, Suppressed Immunity, and Altered Oxidative Metabolism Caused by Pathogenic Microbes in Atherosclerosis and Dementia. *Frontiers in Aging Neuroscience* **9**, 324. ISSN: 1663-4365 (2017).
17. Tinelli, C., Pino, A. D., Ficulle, E., Marcelli, S. & Feligioni, M. Hyperhomocysteinemia as a Risk Factor and Potential Nutraceutical Target for Certain Pathologies. *Frontiers in Nutrition* **6**, 49. ISSN: 2296-861X (2019).
18. Chen, S. *et al.* Homocysteine induces mitochondrial dysfunction involving the crosstalk between oxidative stress and mitochondrial pSTAT3 in rat ischemic brain. *Scientific Reports* **7**, 6932 (2017).
19. Winchester, L. J., Veeranki, S., Givvimani, S. & Tyagi, S. C. Homocysteine elicits an M1 phenotype in murine macrophages through an EMMPRIN-mediated pathway1. *Canadian Journal of Physiology and Pharmacology* **93**, 577–584. ISSN: 0008-4212 (2015).

20. Ma, L. *et al.* Indole Alleviates Diet-Induced Hepatic Steatosis and Inflammation in a Manner Involving Myeloid Cell 6-Phosphofructo-2-Kinase/Fructose-2,6-Biphosphatase 3. *Hepatology* **72**, 1191–1203. ISSN: 0270-9139 (2020).
21. RIDER, M. H. *et al.* 6-Phosphofructo-2-kinase/fructose-2,6-bisphosphatase: head-to-head with a bifunctional enzyme that controls glycolysis. *Biochemical Journal* **381**, 561–579. ISSN: 0264-6021 (2004).
22. Cheung, E. C., Ludwig, R. L. & Vousden, K. H. Mitochondrial localization of TIGAR under hypoxia stimulates HK2 and lowers ROS and cell death. *Proceedings of the National Academy of Sciences* **109**, 20491–20496. ISSN: 0027-8424 (2012).
23. Zhang, W. *et al.* Lactate Is a Natural Suppressor of RLR Signaling by Targeting MAVS. *Cell* **178**, 176–189.e15. ISSN: 0092-8674 (2019).
24. Liu, P. T. *et al.* Toll-Like Receptor Triggering of a Vitamin D-Mediated Human Antimicrobial Response. *Science* **311**, 1770–1773. ISSN: 0036-8075 (2006).

CHAPTER 3

Concluding remarks: implications and future directions

In this final chapter we discuss the major implications of our findings regarding the regulation and splicing of PFKFB3 in response to viral infection and PFKFB3's function in antiviral response. After a brief comment on new evidence regarding the efficacy of PFKFB3 inhibition, we highlight questions arising from this work and possible routes forward.

3.1 PFKFB3 inhibition: many questions to revisit

Presentation or discussion of data from PFKFB3 inhibition studies may seem to have been conspicuously absent here. Small molecule inhibition of PFKFB3 by 3PO has been a key strategy in the study of its function. The transient but significant effects of 3PO and its more potent analogs on glycolysis and angiogenesis have been attributed to successful inhibition of PFKFB3 kinase activity if and when they co-occur with a reduction in the PFK-2 product F-2,6-P. However, the recently-developed inhibitor AZ PFKFB3 67 (AZ67) has made new experiments possible indicating that 3PO does not, in fact, directly inhibit PFKFB3. This is because AZ67 serves as a clearly positive control against which 3PO can be evaluated. AZ67 inhibits the PFK-2 activity of PFKFB3 in in vitro kinase assays and binds to PFKFB3, as measured by isothermal titration calorimetry (ITC) and supported by a crystal structure of AZ67 in the catalytic domain (*1, 2*). 3PO fails to do either. Instead, it appears that 3PO exerts its effects on glycolysis and vessel sprouting via other mechanisms that may include intracellular acidification via accumulation of lactate (*2*).

3PO was recently found to exert an anti-inflammatory effect by inhibiting IKKa/b and JNK phosphorylation even after PFKFB3 silencing in human umbilical cord vein endothelial

cells (HUVECs), and neither PFKFB3 silencing nor the alternative PFKFB3 inhibitor YN1 demonstrated 3PO's anti-inflammatory effect (3). A substantive number of reports include data attributing the effects of 3PO to PFKFB3 inhibition. PFKFB3 knockout causes an embryonic lethal phenotype in mice, so the vast majority of non-inhibitor data available for loss of PFKFB3 activity comes from experiments where PFKFB3 expression is reduced by heterozygosity or RNA interference but not eliminated. There remains, therefore, quite a lot to get to know about PFKFB3 and glycolysis using both newly available PFKFB3 inhibitors and targeted gene knockout strategies.

3.2 PFKFB3, choline and homocysteine converge

We saw dramatic increases in intracellular CDP-choline (over 10-fold) and homocysteine (nearly 100-fold) in cells overexpressing PFKFB3 A-C-G. It's unclear how PFKFB3 activity or increased glycolytic flux might lead to increases in intracellular choline and homocysteine, nor is it clear what the effects of these changes on metabolism or viral infection might be. The accumulation of intracellular CDP-choline does suggest a block in the final step of the Kennedy pathway for PC synthesis. Such a block could lead to decreased PC in cell membranes, but not total loss, because PC can also be formed without need for the Kennedy pathway or even choline availability via transmethylation of phosphatidylethanolamine (PE) to PC by PEMT. This transmethylation reaction requires methionine as a methyl donor, shifting methionine from protein synthesis and potentially limiting viral infection (4).

PEMT is induced by day 5 of 3T3-L1 differentiation into adipocytes (5). Interestingly, PFKFB3 A-C-G is also induced in 3T3-L1 adipocyte differentiation, beginning at day 2 and continuing to increase through day 6. (6) The timing of induction suggests that PFKFB3 could potentially play a role in regulating PEMT expression in this well-defined differentiation condition (3T3-L1 cells are differentiated into adipocytes by culture in the presence of methylisobutylxanthine, dexamethasone, and insulin.) PEMT-deficient mice also have an interesting phenotype because they are protected from high-fat diet (HFD) induced weight gain and insulin resistance but develop fatty livers. On the other hand, PFKFB3 overex-

pressing transgenic mice gained more weight than controls on HFD and developed hepatic steatosis. The striking result from that study from the perspective of the work in Chapter 2 is that Huo et al found that the *conditioned media* from adipocytes overexpressing PFKFB3 could induce hepatic steatosis in cultured hepatocytes.(7)

The ratio of PC to PE is important to membrane function. A lower PC:PE ratio causes membrane permeability and leakage in hepatocytes (8). The PC:PE ratio is also important for stability of lipid droplets, which have single-layer membranes because they enclose neutral lipids. Lipid droplets are fundamental to infection by several viruses, including HCV, which circulates as lipovirions. The HCV nucleocapsid core protein, which coats lipid droplets in the cytosol, activates SREBP-1 and RXR α and downregulates PPAR α to increase lipid synthesis and decrease fatty acid oxidation, ultimately leading to hepatic steatosis in nearly 50% of HCV patients (9). Hepatic steatosis is also caused by problems in diet, often in combination with inborn deficiencies in one-carbon metabolism due to genetic polymorphisms, that may further compound HCV severity: hyperhomocysteinemia and the C677T MTHFR polymorphism associated with increased homocysteine levels both increased prevalence and clinical severity of hepatic steatosis and fibrosis in HCV patients (10). A low-choline diet causes fatty liver and liver damage in humans, with some variation due to genotype and estrogen status (11), and a high-methionine (low choline) diet is used to induce hyperhomocysteinemia and subsequent fatty liver in a mouse model (12).

The effects of PC:PE ratio are due to steric differences between phospholipids that affect membrane morphology: PC is cylindrically shaped and sterically suited to the lamellar structure of lipid bilayers, while PE is more cone shaped and better suited to inverse micelles or micellar tubules (inverse hexagonal phase.) As a result PC is most abundant in the outer leaflet of phospholipid bilayers, while PE is enriched in the inner leaflet and abundant in the cristae of mitochondria. Alterations in PE metabolism have profound effects on the inner mitochondrial membrane and mitochondrial respiration. Meclizine treatment blunts OXPHOS via inhibition of cytosolic cytidyltransferase activity that blocks synthesis of CDP-EtA from P-EtA (13). PE deficiency caused by complete or partial ablation of its mitochondrial synthesis also inhibits OXPHOS, in addition to or because of altering mitochondrial membrane

morphology (14). It's tempting to try to connect PE metabolism to PFKFB3 overexpression because of the association between PFKFB3 and blunted OXPHOS in M1 macrophages and Warburg-like cancer cells, but our metabolomic data shows no significant impact on PE precursors and PE was not measured. It may be that PE concentration in membranes is ill-captured by the relative pool sizes of its precursors, and distribution within the membrane also appears to be particularly important for normal PE function. Recently, Hou et al developed a non-toxic GFP-duramycin probe for PE that could be used to elucidate the effects of PFKFB3 on PE in mitochondrial membranes.(15)

Finding a place for PFKFB3 in the transformations and interrelations that make up choline/ethanolamine and one-carbon metabolism feels a bit like setting up an investigation board with newspaper clippings and string. A clear path forward would be to grow PFKFB3-silenced or stably expressing cells in media containing stable isotope-labelled choline, monitoring incorporation of choline amine carbons into one-carbon metabolism (or other as yet unrecognized shunts) and of choline incorporation into PC via labelled amine nitrogen. Because the carbon components of these pathways are largely replenished by diet, a drug or light-inducible PFKFB3 construct could even be switched on to observe potential re-routing of carbons within the "closed loop."

REFERENCES

1. Boyd, S. *et al.* Structure-Based Design of Potent and Selective Inhibitors of the Metabolic Kinase PFKFB3. *Journal of Medicinal Chemistry* **58**, 3611–3625. ISSN: 0022-2623 (2015).
2. Veseli, B. E. *et al.* Small molecule 3PO inhibits glycolysis but does not bind to 6-phosphofructo-2-kinase/fructose-2,6-bisphosphatase-3 (PFKFB3). *FEBS Letters* **594**, 3067–3075. ISSN: 0014-5793 (2020).
3. Wik, J. A. *et al.* 3PO inhibits inflammatory NF κ B and stress-activated kinase signaling in primary human endothelial cells independently of its target PFKFB3. *PLOS ONE* **15**, e0229395 (2020).
4. Robinson, J. L. *et al.* Dietary methyl donors affect in vivo methionine partitioning between transmethylation and protein synthesis in the neonatal piglet. *Amino Acids* **48**, 2821–2830. ISSN: 0939-4451 (2016).
5. Hörl, G. *et al.* Sequential Synthesis and Methylation of Phosphatidylethanolamine Promote Lipid Droplet Biosynthesis and Stability in Tissue Culture and in Vivo. *Journal of Biological Chemistry* **286**, 17338–17350. ISSN: 0021-9258 (2011).
6. Atsumi, T. *et al.* Expression of Inducible 6-Phosphofructo-2-Kinase/Fructose-2,6-Bisphosphatase/PFKFB3 Isoforms in Adipocytes and Their Potential Role in Glycolytic Regulation. *Diabetes* **54**, 3349–3357. ISSN: 0012-1797 (2005).
7. Huo, Y. *et al.* Targeted overexpression of inducible 6-phosphofructo-2-kinase in adipose tissue increases fat deposition but protects against diet-induced insulin resistance and inflammatory responses. English. *Journal of Biological Chemistry* **287**, 21492–21500 (2012).
8. Vance, D. E., Li, Z. & Jacobs, R. L. Hepatic Phosphatidylethanolamine N-Methyltransferase, Unexpected Roles in Animal Biochemistry and Physiology. *Journal of Biological Chemistry* **282**, 33237–33241. ISSN: 0021-9258 (2007).

9. Camus, G., Vogt, D. A., Kondratowicz, A. S. & Ott, M. Chapter 10 Lipid Droplets and Viral Infections. *Methods in Cell Biology* **116**, 167–190. ISSN: 0091-679X (2013).
10. Adinolfi, L. E. *et al.* Hyperhomocysteinemia and the MTHFR C677T polymorphism promote steatosis and fibrosis in chronic hepatitis C patients. *Hepatology* **41**, 995–1003. ISSN: 1527-3350 (2005).
11. Corbin, K. D. & Zeisel, S. H. Choline metabolism provides novel insights into nonalcoholic fatty liver disease and its progression. *Current Opinion in Gastroenterology* **28**, 159–165. ISSN: 0267-1379 (2012).
12. Yao, L. *et al.* Inhibition of soluble epoxide hydrolase ameliorates hyperhomocysteinemia-induced hepatic steatosis by enhancing β -oxidation of fatty acid in mice. *American Journal of Physiology-Gastrointestinal and Liver Physiology* **316**, G527–G538. ISSN: 0193-1857 (2019).
13. Gohil, V. M. *et al.* Meclizine Inhibits Mitochondrial Respiration through Direct Targeting of Cytosolic Phosphoethanolamine Metabolism. *Journal of Biological Chemistry* **288**, 35387–35395. ISSN: 0021-9258 (2013).
14. Tasseva, G. *et al.* Phosphatidylethanolamine Deficiency in Mammalian Mitochondria Impairs Oxidative Phosphorylation and Alters Mitochondrial Morphology. *Journal of Biological Chemistry* **288**, 4158–4173. ISSN: 0021-9258 (2013).
15. Hou, S., Johnson, S. E. & Zhao, M. A One-Step Staining Probe for Phosphatidylethanolamine. *ChemBioChem* **16**, 1955–1960. ISSN: 1439-7633 (2015).